

# Periodically Spaced Roughness Elements:

## An Investigation of the Possibility to Attenuate Harbor Noise

Master's thesis in the Master's programme in Sound and Vibration

ANNA NOVAK

MASTER'S THESIS BOMX02-16-35

# Periodically Spaced Roughness Elements: An Investigation of the Possibility to Attenuate Harbour Noise

*Master's thesis in the Master's Programme Sound and Vibration*

ANNA NOVAK

Department of Civil and Environmental Engineering  
*Division of Applied Acoustics*  
CHALMERS UNIVERSITY OF TECHNOLOGY  
Göteborg, Sweden 2016

Periodically Spaced Roughness Elements:  
An Investigation of the Possibility to Attenuate Harbour Noise  
Master's Thesis in the Master's programme in Sound and Vibration  
ANNA NOVAK  
Department of Civil and Environmental Engineering  
Division of Applied Acoustics  
Roomacoustics Group or Vibroacoustics Group  
Chalmers University of Technology

## **Abstract**

Roughness elements have previously been used on road traffic noise. In this work the possibility to adapt the roughness elements to harbor noise is examined. Noise emitted from ships tend to be difficult to attenuate, both due to the low frequency content, as well as the fact that the source is highly elevated (by the funnel of the vessel).

To calculate the influence of the roughness elements a 2D Boundary Element Model was created. A primary part of the study is conducted at ground level; here the influences of the different parameters, such as height, width and distance between the canyons are examined. This gives three different configurations tuned to affect the low frequency range of the emitted sound (below 200 Hz). The second part of the study is conducted on the rooftop of a six stories high building. The influence is calculated in three different zones in the neighboring courtyard; at the shadowed and the exposed facade as well as at ear height.

The result showed that it is possible to decrease low frequent noise by using roughness elements. Mainly the height of the elements influences which frequencies are targeted while the width of the canyons influence how broad the targeted frequency range will be. The amount of elements increases the effect.

# Contents

<b>Abstract</b>	<b>2</b>
<b>Contents</b>	<b>3</b>
<b>Acknowledgements</b>	<b>5</b>
<b>1. Introduction</b>	<b>1</b>
1.1. Background . . . . .	1
1.2. Limitations . . . . .	1
1.3. Methodology . . . . .	2
<b>2. The Boundary Element Method</b>	<b>3</b>
2.1. Methodology . . . . .	3
2.2. Gauss-Legendre Quadrature . . . . .	6
2.3. Numerical Implementation . . . . .	6
2.3.1. CHIEF Points . . . . .	8
<b>3. Harbour Noise</b>	<b>9</b>
3.1. Noise Sources of the Harbour . . . . .	9
3.2. Possible Solutions to Harbour Noise . . . . .	10
<b>4. Roughness Elements</b>	<b>13</b>
4.1. Ground Effect . . . . .	13
4.2. Rough Ground . . . . .	14
4.2.1. Surface Wave . . . . .	15
4.3. Roughness Element Parameters . . . . .	16
<b>5. Setup</b>	<b>19</b>
5.1. The Source . . . . .	20
5.2. The Dimensions of the Elements . . . . .	20
5.3. The Courtyard . . . . .	21
5.4. The Calculations . . . . .	21
5.4.1. The Corners and Surface Elements . . . . .	21
5.4.2. Implementation of BEM . . . . .	22
5.4.3. Calculation Data . . . . .	23
5.5. The Evaluation . . . . .	23
<b>6. Validation</b>	<b>25</b>

<b>7. Case Studies</b>	<b>29</b>
7.1. Case Study 1: One Cavity: h and w varies . . . . .	29
7.1.1. Implementation . . . . .	29
7.1.2. Result . . . . .	30
7.1.3. Analysis . . . . .	31
7.2. Case Study 2: Ground Roughness: 2 Elements with Fixed h, w and Varying dd. . . . .	33
7.2.1. Implementation . . . . .	33
7.2.2. Result . . . . .	34
7.2.3. Analysis . . . . .	35
7.3. Case Study 3: Ground Roughness: Increasing the Number of Elements .	36
7.3.1. Implementation . . . . .	36
7.3.2. Result . . . . .	37
7.3.3. Analysis . . . . .	38
7.4. Case study 4: Adding Roughness Elements to the Rooftop. . . . .	38
7.4.1. Implementation . . . . .	38
7.4.2. Result . . . . .	41
7.4.3. Analysis . . . . .	44
<b>8. Summary</b>	<b>45</b>
<b>References</b>	<b>47</b>
<b>A. Matlab-code</b>	<b>51</b>

# Acknowledgements

I would like to thank everybody at the department of Technical Acoustics at Chalmers. A special thanks to Bart van der Aa, Jens Forssen, Wolfgang Kropp, Gunilla Skog and Borje Wijk.

I would also like to thank my friends for the love and the support ♡ ( $\nabla^2 = \Delta$ ).



# 1. Introduction

In this thesis the Boundary Element Method (BEM) is formulated and applied to study sound propagation over roughness elements. The roughness elements are modelled to adjust the ground effect so that an investigated frequency range will be attenuated.

**The purpose is to investigate whether periodically spaced roughness elements can be adapted in order to mitigate harbour noise.**

The reason for the study is to see if roughness elements can be an efficient solution for preventing noise generated by a cruise ship from propagating to the neighbouring residence areas. The idea is to introduce a noise reduced zone in the courtyards. Studies have shown that tenants are less likely to be disturbed by noise if the habitable rooms of the apartments are connected to a noise reduced zone.

The study is divided into two parts. At first it is conducted at ground level. Thereafter, based on the result from the first case study, the roughness elements are placed on the rooftop of a six floor high residence building. The sound pressure level in the courtyard is compared for the case with and without the elements at the rooftop. This is conducted by calculating the Insertion Loss.

## 1.1. Background

Previously the effect of ground roughness has been studied for mitigation of road traffic noise as well as for airport induced noise. Studies have examined the effect of the dimensions and periodic distribution of the elements, as well as the effect of added vegetation in connection with the elements.

## 1.2. Limitations

The study investigates a 2-dimensional case. No meteorological parameters such as wind, humidity, and temperature gradients have been taken into consideration. A homogeneous medium is therefore assumed throughout.

Only one source position have been used for each case.

To shorten the computational time of the calculations the facades of the buildings are assumed to be flat.



### **1.3. Methodology**

The work consists of a continuous literature study which is combined with firstly a comprehension process of the provided method. The literature study also examines harbour noise and looks at previous studies of roughness elements

A BEM-model is developed and validated against both a Finit Element Model and existing results from studies conducted on surface roughness at ground level. The optimization process (to adjust the roughness elements depending on the frequency range) is first conducted at ground and later applied to a rooftop of a residential building. The size and the number of the roughness elements are adjusted to increase the achieved noise reduction in the courtyard for a certain frequency range.

## 2. The Boundary Element Method

How scattering from an arbitrarily shaped object affects the incoming sound wave is a commonly occurring problem in acoustics. For some elementary objects with simple shapes analytical solutions exist [1]. However for objects with more complex shapes the use of numerical methods such as the Finite Element Method (FEM) or the Boundary Element Method (BEM) are necessary. In this work we will focus on the BEM.

The BEM is conducted by first converting the Partial Differential Equation (PDE), which formulates the problem into an Integral Equation (IE) which later on is discretized. The IE is seen as an exact solution of the PDE. The most commonly used PDE is the continuous Kirchhoff-Helmholtz Integral Equation [2]. Here the PDE which governs the solution in the whole domain is replaced by an IE that only governs the solution at the boundary, in other words a Boundary Integral Equation [3]. Now any object in space can be described as a set of secondary sources. Once the amplitudes of the secondary sources are calculated the total pressure field at any desired position in the surroundings of the scattering object can be calculated with the IE.

The advantage with the BEM compared to the FEM is that in BEM only the boundary is discretized instead of the whole domain. This is beneficial for radiation and scattering problems which might be extending infinitely in one or many directions.

### 2.1. Methodology

Assume an object with an arbitrary shape and a closed contour line  $S$ . The object is situated in free space  $D$ , see figure (2.1).

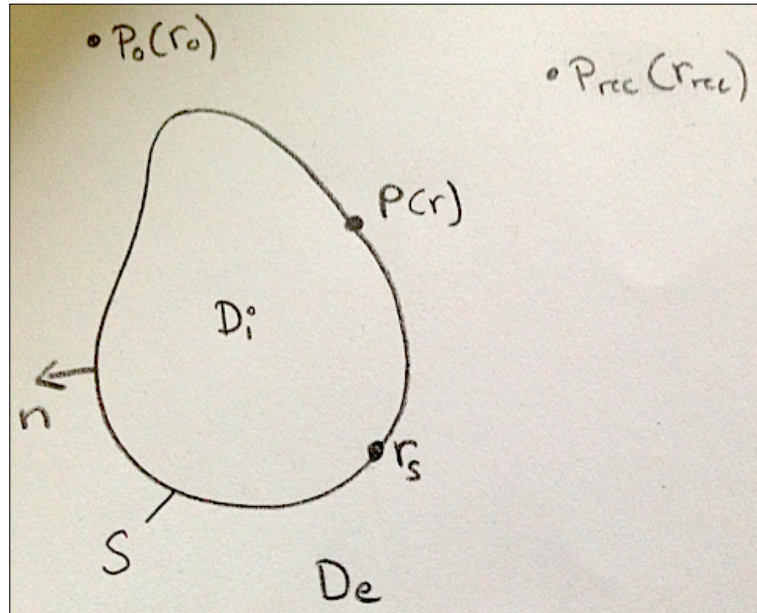


Figure 2.1.: The figure shows an arbitrary shaped object. The exterior domain is denoted  $D_e$ , while  $D_i$  is the interior domain and  $S$  the boundary or the surface.  $p_0$  is the pressure from a source positioned at  $\vec{r}_0$  and  $p$  the pressure at a position at the boundary  $\vec{r}$ ,  $\vec{r}_s$  is also a position at the surface.  $p_{rec}$  is the pressure at a receiver position  $\vec{r}_{rec}$ .

The object is insonified by a source  $p_0$  positioned at  $\vec{r}_0$ . The pressure field from the source is known.

When conducting the BEM we will reformulate the original Helmholtz Equation (our PDE) as a Boundary Integral Equation (BIE). In the BIE the integral will be taken over the surface of the object. Here follows the Helmholtz Integral Equation at the surface

$$\frac{1}{2}p(\vec{r}) = \int_S \left( p(\vec{r}_s) \frac{\partial g(\vec{r}, \vec{r}_s)}{\partial n} - g(\vec{r}, \vec{r}_s) \frac{\partial p(\vec{r})}{\partial n} \right) dS. \quad (2.1)$$

where  $n$  is the normal direction of the surface  $S$  directed towards the exterior domain  $D_e$  and  $g(\vec{r}, \vec{r}_s)$  is the Green's function from any point on the surface to each point on the surface and  $\frac{\partial}{\partial n}$  is the partial derivative in normal direction to  $S$ . Assume the time convention  $e^{j\omega t}$  is followed.

The solution to the Integral Equation depends on the location of the receiver point  $p(\vec{r})$ . If the receiver is positioned at  $D_e$ , at  $S$  or inside  $D_i$  following equation yields

$$\int_S \left( p(\vec{r}_s) \frac{\partial g(\vec{r}, \vec{r}_s)}{\partial n} - g(\vec{r}, \vec{r}_s) \frac{\partial p(\vec{r}_s)}{\partial n} \right) dS = \begin{cases} p(\vec{r}) & \vec{r} \in D_{\text{exterior}} \\ \frac{1}{2}p(\vec{r}) & \vec{r} \in S \\ 0 & \vec{r} \in D_{\text{interior}} \end{cases} \quad (2.2)$$

It represents either the Exterior Helmholtz Integral Equation (EHIE), the Surface Helmholtz Integral Equation (SHIE) or the Interior Helmholtz Integral Equation (IHIE)[4]. In this work we will examine scattering from an object, therefore the problem will only be solved outside  $D_i$  [5].

To solve the SHIE we need to find the boundary conditions e.g. the pressure and the normal velocity at the surface of the object. Consider the exterior Neumann problem

$$\frac{\partial p}{\partial n} = -j\omega\rho_0 v_n \quad (2.3)$$

where  $\frac{\partial p}{\partial n}$  is the partial derivative of the pressure in normal direction,  $\omega$  is the angular frequency,  $\rho_0$  is the density of air and  $v_n$  is the velocity in normal direction. Combined with the specific impedance condition

$$Z = \frac{p}{v_n} \quad (2.4)$$

and the normalized admittance

$$\beta = \frac{\rho c}{Z} = \rho_0 c \frac{v_n}{p} \quad (2.5)$$

we get following boundary condition at the surface  $S$ ,

$$\frac{\partial p}{\partial n} = -jk\beta p \quad (2.6)$$

where

$$k = \frac{\omega}{c} \quad (2.7)$$

is the wave number with  $c$  as the speed of sound in air [6].

When combining equations (2.2) and (2.6), following expression will be obtained

$$p(\vec{r}) = - \int_S p(\vec{r}_s) \left( jk\beta g(\vec{r}, \vec{r}_s) + \frac{\partial g(\vec{r}, \vec{r}_s)}{\partial n} \right) dS, \quad \vec{r} \in D_{\text{exterior}} \quad (2.8a)$$

$$\frac{1}{2}p(\vec{r}) = - \int_S p(\vec{r}_s) \left( jk\beta g(\vec{r}, \vec{r}_s) + \frac{\partial g(\vec{r}, \vec{r}_s)}{\partial n} \right) dS, \quad \vec{r} \in S \quad (2.8b)$$

$$0 = - \int_S p(\vec{r}_s) \left( jk\beta g(\vec{r}, \vec{r}_s) + \frac{\partial g(\vec{r}, \vec{r}_s)}{\partial n} \right) dS, \quad \vec{r} \in D_{\text{interior}} \quad (2.8c)$$

The Green's function is the fundamental solution to the Helmholtz Equation. For a two-dimensional problem treated here the Greens function is based on the Hankel function  $H_0^{(1)}$  of 0<sup>th</sup> order and 1<sup>st</sup> kind. The Hankel function is convenient to use for an unbounded wave problem. Since we only look at outward propagating waves it can be expressed as following.

$$g(\vec{r}, \vec{r}_s) = \frac{i}{4} H_0^{(1)}(kr) \quad (2.9)$$

with the derivative

$$\frac{\partial g(\vec{r}, \vec{r}_s)}{\partial n} = -\frac{ki}{4} H_1^{(1)}(kr) \quad (2.10)$$

where  $r$  is the distance between the two points  $\vec{r}$  and  $\vec{r}_s$  [7].

## 2.2. Gauss-Legendre Quadrature

To approximate the integral at the boundary of the object, a numerical integration method will be used. Here the Gauss-Legendre quadrature is chosen. The quadrature is based on

$$\int_{-1}^1 f(x) dx = \sum_{i=1}^N w_i f(z_i) \quad (2.11)$$

where  $f(x)$  is the function over the interval  $[1,-1]$ ,  $z_i$  are the abscissas (position of the nodes) and  $w_i$  are the corresponding weights. In Gauss-Legendre quadrature both the nodes and the weights are chosen (e.g. the nodes does not need to be equally spaced). The integral is approximated as the weighted sum of  $N$  function evaluations. By applying the Gauss-Legendre quadrature to the Surface Helmholtz Integral Equation transforms into a system of linear equations.

Here the 10<sup>th</sup> order Gauss-Legendre quadrature is used.

## 2.3. Numerical Implementation

For a numerical solution to the 2-dimensional Surface Helmholtz Integral Equation (SHIE), the boundary is discretized into  $M$  constant surface elements  $m = 1, 2, \dots, M$ . Each element is surrounded by two end points. At the centre of each element lies a node, see figure 2.2. The pressure  $p$  and normal velocity  $\frac{\partial p}{\partial n}$  is considered to be constant over each single surface element [4].

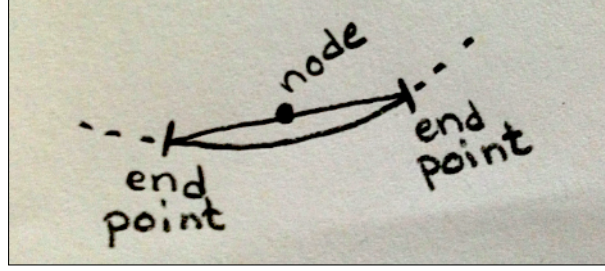


Figure 2.2.: Each surface element is surrounded by two end points and at the centre of each element lies a node.

A point  $r_i$   $i = 1, \dots, M$  is positioned at the node of each surface element. The contribution from all other elements to each element will form  $M$  different equations for each surface element. By using the Gauss-Legendre quadrature to evaluate the integrals the discretized version of the SHIE yields

$$C(\vec{r}_i)p(\vec{r}_i) = - \sum_{m=1}^M \left( p(r_m) \frac{\partial g(\vec{r}_i, \vec{r}_m)}{\partial n} + jk\beta g(\vec{r}_i, \vec{r}_m) \right) \Delta S_m + p_o(\vec{r}_i). \quad (2.12)$$

where  $g(\vec{r}_i, \vec{r}_m)$  denotes the Green's function from element  $m$  to  $i$  and  $\Delta S_m$  the boundary element patch.  $p(r_i)$  is the pressure at the element  $i$  due to the contribution from all other nodes on the surface and  $p_o(\vec{r}_i)$  the contribution from the source at patch  $i$ .  $C$  is a constant which differ according to equation 2.2.

For the case where  $m = i$  the integration will be performed over a singularity. How this can be resolved is described by [9]

By sorting the unknown parts of equation 2.12 to the right hand side and the known parts to the left hand side the matrix equation can be formulated as

$$\mathbf{b} = \mathbf{A}\mathbf{x} \quad (2.13)$$

where the unknown boundary values at the surface can be found in  $\mathbf{x}$ . This can numerically be expressed as

$$\begin{bmatrix} p_{o,1} \\ p_{o,2} \\ \vdots \\ p_{o,M} \end{bmatrix} = \begin{bmatrix} \frac{1}{2} + \gamma_{1,1} & \gamma_{1,2} & \dots & \gamma_{1,M} \\ \gamma_{2,1} & \frac{1}{2} + \gamma_{2,2} & \dots & \gamma_{2,M} \\ \vdots & \vdots & \ddots & \vdots \\ \gamma_{M,1} & \gamma_{M,2} & \dots & \frac{1}{2} + \gamma_{M,M} \end{bmatrix} \begin{bmatrix} p_1 \\ p_2 \\ \vdots \\ p_M \end{bmatrix} \quad (2.14)$$

where the right hand side is the vector with the unknown boundary pressures of each element  $i$  while the matrix contains the contribution from all other elements. The left hand side contains the contributions from the source.

Each element at the surface can be seen as a secondary source contributing to the scattered field. When the pressure and the normal velocity are known on  $S$ , these can be used to numerically calculate the pressure field at every point within  $D_{exterior}$  [9].

### 2.3.1. CHIEF Points

If the frequency of the incident wave coincides with a resonance frequency of  $D_{interior}$ , there will be more solutions to the problem than one. The solution will therefore not be unique and will thereby cause instability. In case of instability the results start to oscillate and will provide incorrect values. To avoid this the Combined Helmholtz Integral Equation Formulation (CHIEF) is applied. It is a technique devised by [10] and takes advantage of that the Interior Helmholtz Integral Equation (IHIE) will give a null-field in  $D_{interior}$ . Knowing that the pressure inside the object should be zero the correct solution can be obtained.

$$p(\vec{r}_o) - \int_S \left( g(\vec{r}, \vec{r}_o) \frac{\partial p(\vec{r})}{\partial n} - p(\vec{r}) \frac{\partial g(\vec{r}, \vec{r}_o)}{\partial n} \right) dS = 0 \quad (2.15)$$

The idea is to place a number of additional points inside  $D_{interior}$  for which the IHIE must be satisfied [9]. This will lead to an overdetermined system of equations. The position of the CHIEF-points are placed randomly to avoid the risk of all of them being positioned on e.g. nodal points of the interior mode within the domain.

## 3. Harbour Noise

As seen today in Sweden (as well as in other countries) harbour areas are giving up space for new residences, as a part of the urbanization [11]. Still the harbour is an important source, not only for the supply of goods but as well for tourism. Therefore making them important for the city's development [12]. The consequence of this is that the distance between the dwellings and the harbours continue to decrease. More dwelling areas will then be exposed for the noise emitted by the harbours.

### 3.1. Noise Sources of the Harbour

In their article [17] divides the noise sources of a vessel or a ship according to their activity as follows:

- when the ship sails along the coast it is the exhaust from the main propulsion engines which are the main contributors of the emitted noise.
- when the ship is entering or exiting the harbour it is the manoeuvring equipment which causes most noise.
- when the ship is at quay it is no longer the main engine which are running but the auxiliaries. As well will noise be emitted from operating cranes, ramps and other activities due to charging/discharging the ship.

The emitted noise from the ports can be divided into **direct noise** and **indirect noise** according to [13]. Noise emitted from the ships when entering and leaving the port or being moored is an example of direct noise. While noise emitted from activities related to the presence of the ship, like loading/unloading and restoration work are categorized as indirect noise. Characteristics for indirect noise is impact noise from e.g. slamming or accelerating engines. Characteristics for direct noise is steady low-frequency noise. The main contributor to the noise climate in the port is the direct noise [13].

The characteristics of the direct noise differ from vessel to vessel. However the exhaust of the main and auxiliary engines is the most important contributor of airborne noise [16]. The outlet is placed by the funnel at the top of the vessel[17]. Contributing are as well the inlets and outlets of the ventilation system [16], [17]. Figure 3.1 shows typical positions of the sources.





Figure 3.1.: The main contributors of the direct airborne noise are marked with black.

Different sources has different frequency content. When being moored the main engines are turned of and only the auxiliary engines are running. For vessels like ro-ro, ro-pax and ferries the auxiliary engines run the ventilation system from the garage. For cruise ships the HVAC system which regulates the climate in the cabins is running continuously [13]. For the fans the frequency content of the sound power is mainly in the intermediate frequency range, around 250 - 2000 Hz [11]. The majority of the noise from the engine exhaust is at low frequencies below the 250 Hz octave band [14].

The noise from the main engines is the most troublesome. It is not only difficult to attenuate due to the low frequency content but as well is the location of the source at the funnel highly elevated [15].

### 3.2. Possible Solutions to Harbour Noise

There is no standard ship, they all have different sizes and engines and they move all over the world. It is therefore difficult to decide who is responsible for the noise from the vessels. Will it be the shipping company or the harbour, and how can the harbour itself regulate the noise emitted from ships without disturbing the supply of goods or tourism?

The harbour itself can adjust the indirect noise by e.g. improving ramps, adding silencers to the ground vehicles, keeping the ground surface smooth and flat, adjusting

the route for the arriving vehicles so that they have to keep the speed down and not accelerate. It is possible to improve the indirect noise while the direct noise is more difficult to decrease since it is not always known which ships will enter the harbour.

For ships which frequently visit the same harbour shore power could be a solution for decreasing the emitted noise. According to [18] the sound reduction due to shore power is more or less efficient depending on the type of ship. Most efficient sound reduction is achieved for bulk and general cargo ships. For tankers and RoRo-ships where the ventilation of the cargo deck and the pumps are active while being moored the on shore power will not be as efficient for reducing noise. For the air quality however the shore power may have a great benefit [18]. The problem is however technical difficulties since there is no standard for the power used on board ships. A standardization process is however in progress according to [11]. To decrease the emitted noise from the vessels [11] suggests that the ships could be berthed with the less noisy side towards the dwelling areas. They also suggest that ships should only be able to enter the port if they provide data on measurements of the noise radiated from the vessel. If this is not done, or if the measurement data exceeds a certain limit, the ships may be charged with a fee for berthing.

These are options that could help the harbour to keep the sound levels down. Another possible solution is to work with urban planning. According to [19] studies have shown that noise disturbance decreases if an apartment has a connection to a noise reduced zone to which the habitable rooms are directed. The study was however made on road traffic noise and not harbour noise.



## 4. Roughness Elements

The prevention of unwanted noise from propagating into areas for dwellings and recreation can be done in different ways. A traditional solution for noise reduction is the usage of barriers. In this work however we examine an alternative solution, ground roughness.

The idea with roughness elements at ground is to adjust the ground effect. The elements can be optimized to attenuate the frequencies where most energy is generated by the source [20].

A benefit with ground roughness compared to noise barriers, is that roughness elements are efficient both when the source (or receiver) is close or far away. Noise barriers instead are more efficient the closer they are to the source. Another benefit is that the line of sight between the source and the receiver does not need to be blocked. Therefore the visual impact on the urban environment can be decreased. The roughness elements could e.g. be applied next to highways and therefore reduce the feeling of driving in a tunnel (which can be a negative effect of using barriers). Roughness elements next to highways have been investigated by [22] and shown beneficial results for reducing road traffic noise.

Ground roughness can also be designed to reduce low frequencies which are difficult to restrain with screens or walls (this is due to the long wavelength at these frequencies)[21]. It could also be possible to add the roughness elements on roof tops of garages, airports or dwellings [23]. The benefit is that less space will be occupied. However then the maintenance point-of-view needs to be considered.

### 4.1. Ground Effect

The interference between the direct sound wave and the reflected sound wave is referred to as the ground effect [24]. By adding roughness elements and creating an unsmooth surface it is possible to adjust the first destructive interference between the direct path  $R_1$  and the reflected path  $R_2$ , see figure 4.1.

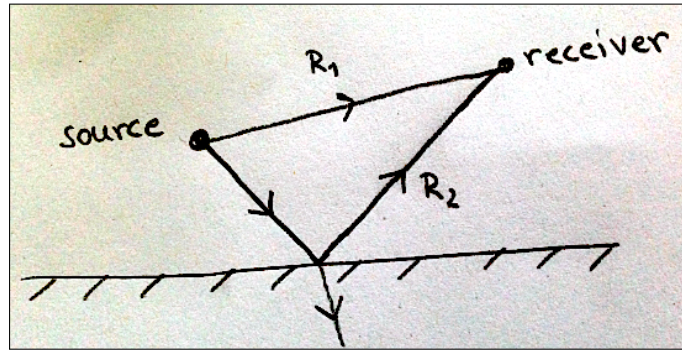


Figure 4.1.: The different paths for the direct and the reflected sound wave.

For hard ground the maximum attenuation due to the ground effect occurs when an odd multiple of half the wavelength  $\lambda$  of the propagating wave corresponds to the difference in path length between the direct and the reflected sound wave [23]. For distances  $R_1$  and  $R_2$  the first destructive interference occurs at following frequency

$$f = \frac{c_0}{2(R_2 - R_1)} \quad (4.1)$$

where  $c_0$  is the speed of sound in air.

For a smooth hard ground the first destructive interference usually occurs too high in frequency to be of interest when looking at sound reduction in outdoor sound propagation [25]. By adjusting the ground the destructive interference could instead occur at a targeted frequency range.

## 4.2. Rough Ground

The flow resistivity is a measure which describes how easily air can move in and out of the ground. If the ground surface has a high flow resistivity it is difficult for air to flow through the surface. When the porosity of a surface increases then the flow resistivity decreases [25].

Reflections on a porous ground will not only lead to a possible reduction of the magnitude of the reflection, it will as well lead to a phase shift (time-delay) due to the finite ground impedance. When a surface becomes rough the effective flow resistivity of the surface decreases. A rough surface is always considered to have a finite impedance [25], [27]. Some of the energy will also be converted into heat [29]. For these reasons the first destructive interference can occur at lower frequencies than for a non-porous surface. According to [26] studies also show that a wider range of frequencies are affected by the first destructive interference when the surface is rough compared to a flat surface.

It is important according to [20] and [28] that the dimensions of the elements are smaller than the wavelength  $\lambda$  of interest. The ground elements under study are only defined as roughness elements when the width  $w$  and depth  $d$  are smaller than the wavelength of the propagating sound wave. This can be expressed as following

$$kw \simeq kd \lesssim 1 \quad (4.2)$$

where  $k$  is the wave number. When the dimensions are sufficiently small the ground will allow coherent scattering. If the dimensions becomes to big the incoherent scattering will dominate and then the ground interference effects are destroyed [20].

The quarter wave resonator is mentioned in [27] as a contributor to the reduction of the sound field. However it later shows to be of small importance. Instead they mention diffraction gratings effects and interference between the direct and the multiple reflected paths which passed through the canyons between the elements. Both are parts of the diffraction assisted ground effect. Especially at high frequencies the diffraction is responsible for the attenuation according to [23].

The different contributions to the total sound field at a receiver point can be divided into following parts[24]

$$P_{total} = P_{direct} + P_{refracted} + P_{surface} \quad (4.3)$$

Equation 4.3 shows that there are three main mechanisms which influence the propagating sound wave. Interference between the propagating sound waves will be one of the consequences as well as the creation of a surface wave [23]. According to [29] if the surface is acoustically hard, the likelihood that the roughness induces a surface wave is increased.

#### 4.2.1. Surface Wave

For a hard smooth surface the impedance is considered to be infinite. Adding texture to the surface and making it rough will change the impedance to finite value [25], [27]. When the reactive part (the imaginary component) is greater than the resistive part (the real component) a surface wave can occur [24], [30]. When the reactive component of the impedance is greater it also means that the flow resistivity is lower [23].

The surface wave is described as the air particles which propagate in an elliptical motion along the surface, or the impedance boundary [21]. The movements is a combination of a parallel motion along the surface and a motion in and out of the cavities in direction normal to the surface [25] [27]. It decays slower than the other components [25], [21]. When the flow resistivity is low the effect of the surface wave is greater.

[24] measured the Excess Attenuation (EA) for randomly distributed roughness elements and periodically spaced roughness elements and found out that a stronger sur-

face wave is excited for periodically spaced roughness elements (both having the same mean spacing excited). They also found that a smaller center to centre spacing between the elements produced a stronger surface wave.

According to [23] a surface wave is more likely to be generated if the number of edges are increased or if the source height decreases and comes closer to the grazing angle. There is a minimum number of cavities needed for the wave to be able to propagate [27]. By modulating the height and the centre-to-centre spacing of the cavities it is possible to adjust the amplitude of the surface wave contribution and which frequencies that are targeted by it[24].

At certain receiver positions and in the lower frequency range the generation of the surface wave could be responsible for negative attenuation [23], i.e. the sound field could be amplified compared to the case if the surface wave was not generated. This can be seen as that the sound is trapped in the vicinity of the surface [27].

In [22] the addition of absorptive material in the canyons is proved to reduce the surface wave generation. If the occurrence of the surface wave is reduced it will according to [23], [27] lead to a reduction of the noise.

### 4.3. Roughness Element Parameters

We will now focus on which parameters influence the result and move the occurrence of the ground effect lower in frequency. The following physical parameters are according to [23] of importance for the resulting sound field and the propagation of the sound wave over roughness elements:

1. the wavelength of the incident wave,  $\lambda$
2. the depth of the cavity,  $d$
3. the width of the cavity,  $w$
4. the total number of diffracting elements
5. the source and receiver locations
6. the shape of the roughness elements
7. the overall distance covered by diffracting elements

The previous section explains the first five parameters to be of influence.

[24] examines how different shapes of the roughness influences the performance of the Excess Attenuation (EA). A high EA is a measure of a high noise reduction. According to [24] tall rectangles and square strips give the best EA at lower frequencies. The study also shows that as the roughness height increases the first EA maxima as well increase in magnitude and become sharper.

For the second EA maxima, studies made by [20] and [24] explains that it is the centre-to-centre distance between the elements that influences the appearance of the second peak. When the distance increases the peak becomes wider. According to [24] there is a linear relationship between the wavelength of the incoming sound wave and the centre to centre distance, for a certain EA.

The third EA maxima is said to be dependent of the percentage of exposed surface between the elements. In studies made by [24] they discover a third EA maxima when 50 % or more of the surface is exposed by the roughness canyons i.e. the percentage of the rectangles covering the ground is 50 % or less. The study also shows that the third EA maxima will move towards lower frequencies when the source and receiver height is increased.

In a study made by [31] the coupling between the elements is shown to increase when the canyons are placed closer to each other.

[20] shows that an increase of the number of semi cylinders also improves the result. More energy will then be trapped in the cavities.

According to [23], under a certain frequency the EA is related to the depth of the element canyon. After a certain frequency the distance between the edges will be the important factor on the performance of the excess attenuation.

Periodic spacing shows according to [32] give deeper relative SPL minima than random spacing. According to [24] periodic spacing will result in a multiple distinct EA maxima while random spacing results in a broader EA maxima.





## 5. Setup

Three different case studies will examine how height, spacing, width and amount of the elements influences the result. These case studies are conducted at ground level. The goal is to find a pattern or a set up which is beneficial for noise reduction, and which can be applied to a rooftop. The only constraint is that the total width of the roughness elements should not exceed the width of the building.

For the first three case studies the source is placed at ground level to avoid the influence of the ground interference. It is positioned 50 m from the first object, see figure 5.1.

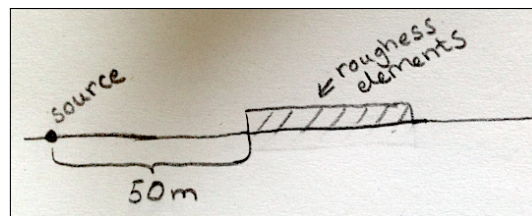


Figure 5.1.: The position of the source compared to the roughness elements.

Later on a fourth case study will be conducted. The set up of the elements will be based on the result from the first three cases studies. In case study number four the elements are placed on the rooftop of a 19.2 m high building. When the study is conducted on the rooftop the source is positioned at a height of 30 m, 100 m away from the first building, see figure 5.2. These conditions were chosen to simulate a typical situation of a ship passing or being moored close by a residential building.

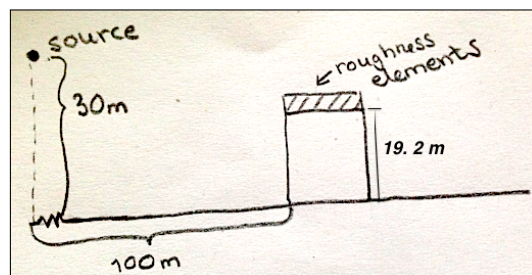


Figure 5.2.: The position of the source compared to the roughness elements.

## 5.1. The Source

A sound power spectrum made-up to model a typical 200 m long cruise ship is provided from the consultancy company Structor Akustik AB. The spectrum is based on measurements from a number of different cruise ships, see figure 5.3.

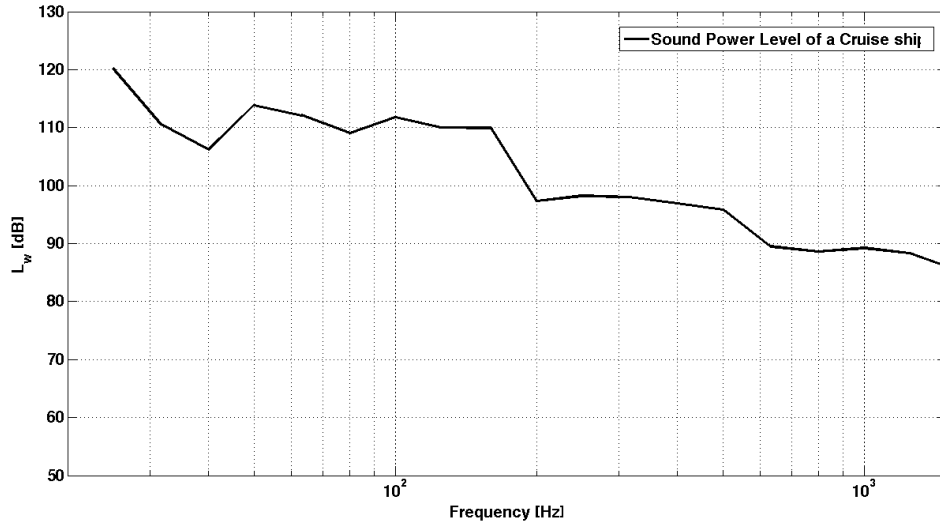


Figure 5.3.: Assumed sound power spectrum of an average 200 m long cruise ship

As seen from the spectrum most energy is generated below 200 Hz. Therefore, in this work, we will focus on the frequency range 31.5 - 200 Hz, here denoted as the low frequency region. It also coincides with the low frequency range for which there are regulations on the sound pressure level indoors in Sweden according to [34].

## 5.2. The Dimensions of the Elements

The parameter for the dimensions of the elements will be called  $q$ .  $q$  is related to a chosen target frequency, in this case 100 Hz. To match the frequency range where the noise from the cruise ships are most dominant the dimensions of the canyons are related to the quarter wavelength of the target frequency. According to [23] the first quarter wave resonance is found when the height of the cavity fulfils the following equation.

$$q = (2n + 1) \frac{\lambda}{4} \quad (5.1)$$

If the target frequency is set to 100 Hz, then  $\lambda=3.4$  m. If  $n = 0$ , then  $q = 0.85$  m.

Since 100 Hz is just a chosen frequency we will also investigate what happens if  $q$  varies. What will be the result if  $q$  decrease ( $q/2$ ), or increase ( $2q$ )?

### 5.3. The Courtyard

The effect of roughness elements placed on a rooftop will be investigated. The set up of the buildings and the courtyard are taken from [33], see figure 5.4.

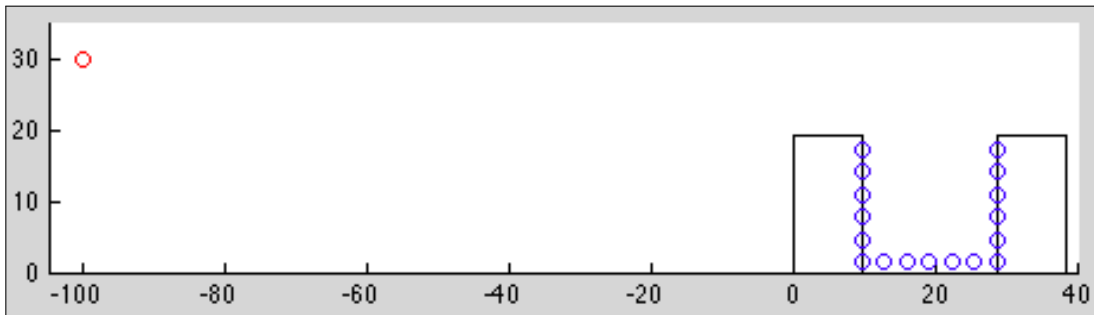


Figure 5.4.: The set up of the courtyard. The red circle is the position of the source and the blue circles are the receiver positions.

The width of one building is 9.6 m and the height is 19.2 m. The distance between two buildings (the size of the courtyard) is 19.2 m. The blue and red circles shows the positions of the source and the receivers, this will be described more in detail in chapter 7.4. To shorten the computational time of the calculations the facades are assumed to be flat and rigid in this study.

### 5.4. The Calculations

Depending on if the study is conducted at ground level (case study 1-3) or at the rooftop (case study 4), two different MATLAB-codes are used to draw the corners and nodes of the roughness elements. The performance of the BEM is however the same for all case studies.

#### 5.4.1. The Corners and Surface Elements

At first the corners of the elements above ground (when  $z \geq 0$ ) are assigned, see figure 5.5. The corners are then mirrored in the  $x$ -plane.

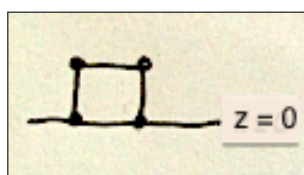


Figure 5.5.: The corners of the element are assigned above ground ( $z \geq 0$ ).

The mirroring is then done in two different ways. When the roughness elements are positioned at ground level all corners above ground are mirrored at the same time, see

explanation in figure 5.6.

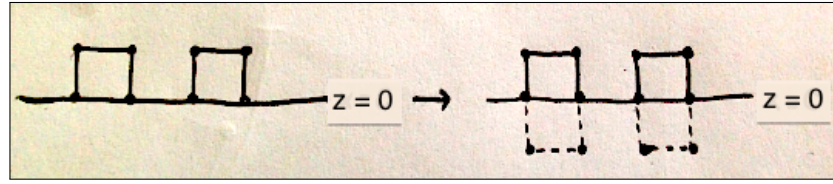


Figure 5.6.: When the study is conducted at ground all roughness elements are mirrored in the x-axis all at the same time.

When the roughness elements are placed on the rooftop of the courtyard, each building is mirrored separately, see figure 5.7.

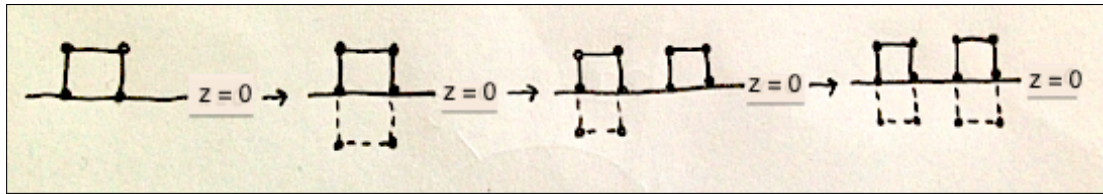


Figure 5.7.: When the study is conducted at the rooftop each building is mirrored in the x-axis separately.

Each surface element of the object is then discretized into  $N$  small patches with a node and a unit vector is assigned to each patch. The unit vector gives information in which direction the path will be drawn. The number of patches is calculated as

$$N = \frac{l}{d_l} \quad (5.2)$$

where  $l$  is the length of a side of a roughness element and  $d_l$  is the size of each patch which is decided by

$$d_l = \frac{c_0}{f_{max} N_{ppw}} \quad (5.3)$$

where  $c_0$  is the speed of sound,  $f_{max}$  is the highest calculated frequency and  $N_{ppw}$  is the number of points per wavelength in the spatial sampling.

This procedure is done for all roughness elements.

#### 5.4.2. Implementation of BEM

The implementation is done as described in chapter 2.3. The following calculations are performed for each of the  $N$  surface elements.

First a node is positioned in the centre of each of the  $N$  surface elements. The positions of the center nodes are found by using the Gauss-Legendre quadrature. In the next step the distance from the source position to each node on the surface, as well the distance from the image source to each node is calculated. The distance from one node to all other nodes on the surface is also needed.

The assigned values for the Green's functions are given in equation 2.1 - 2.1.

The surface pressures can now be found by solving the matrix in equation 2.14 and applying the source as in equation ???. No source spectrum has been applied to the source.

The exact same procedure is done for each chief point inside  $D_i$  as for the surface elements. The MATLAB-codes are found in the Appendix.

### 5.4.3. Calculation Data

The following parameters, see table 5.1, have been used in the calculations.

Table 5.1.: Parameters used in the calculations of Case Study 1 - 3 and 4.

Parameter:	Case Study 1-3:	Case Study 4:
$N_{ppw}$	20	10
$f_{max}$	1120	708
$d_l$	0.015	0.048
$N_{chief}$	8 per roughness element	16 in total for 2 buildings
Order of Gauss-Legendre quadrature	10	10

Due to the long computational time for case study 4 some parameter simplifications have been made. However the validation will show that the calculations are still accurate.

## 5.5. The Evaluation

The Insertion Loss (IL) is a value for the loss due to an added object. Since we are interested in the result of the canyons of the roughness elements and not the results on the element height, the IL will be compared to a box with the same outer dimensions in each case. In this way we eliminate the result due to shading. The IL is calculated as

$$IL = 20 \log \left( \left| \frac{p_{box}}{p_{roughness}} \right| \right) \quad (5.4)$$

where  $p_{box}$  is the case without added roughness and  $p_{roughness}$  is the case with.

When calculations are conducted at ground level the result at the receiver will be averaged over four different receiver positions. Also the receivers are positioned at ground level, just like for the source. The receivers are placed at a distance of 2.1, 3, 3.5 and 4 m away from the last roughness element. The average IL is taken between 31.5-200 Hz and compared between the different case studies.

For case study 4 the IL is compared to the Sound Pressure Level (SPL) of the source spectrum, see figure 5.3. The change in distance between the 17 different source positions is not taken into consideration. The results are all compared to the SPL calculated at a distance of 100 m from source.

## 6. Validation

The two different MATLAB-codes for the Boundary Element Method are validated against a case taken from [20]. The same case is also calculated with the Finite Element Method by using the software Comsol Multiphysics. As explained in chapter 5.4 the nodes of the surface elements are drawn in two different ways. Therefore both MATLAB-codes are validated. They are called *BEM ground* and *BEM rooftop*.

The set up which is taken from [20] consists of a source and a receiver placed 3 m away from each other at a height of 0.131 m. In the middle of them lies roughness elements. They have a height and width of 0.1 m and are placed with a distance of 0.1 m. The setup is calculated with 5 and 15 elements above ground. See figures 6.1 and 6.2. The elements can also be called bosses.

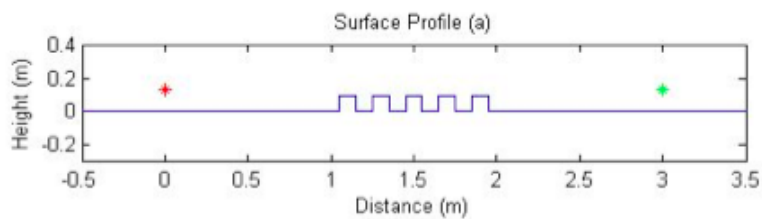


Figure 6.1.: Validation set up with 5 square elements above ground placed between the source and the receiver. Figure taken from [20].

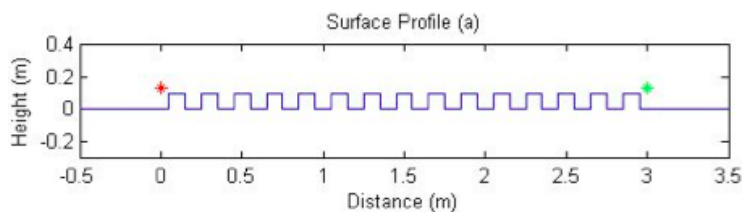


Figure 6.2.: Validation set up with 15 square elements above ground placed between the source and the receiver. Figure taken from [20].

The results from the calculation are shown in 6.3 and 6.5. These results can be compared to the result from [20] shown in figure 6.4 and 6.6 where the blue curve (called a) is the one of interest.



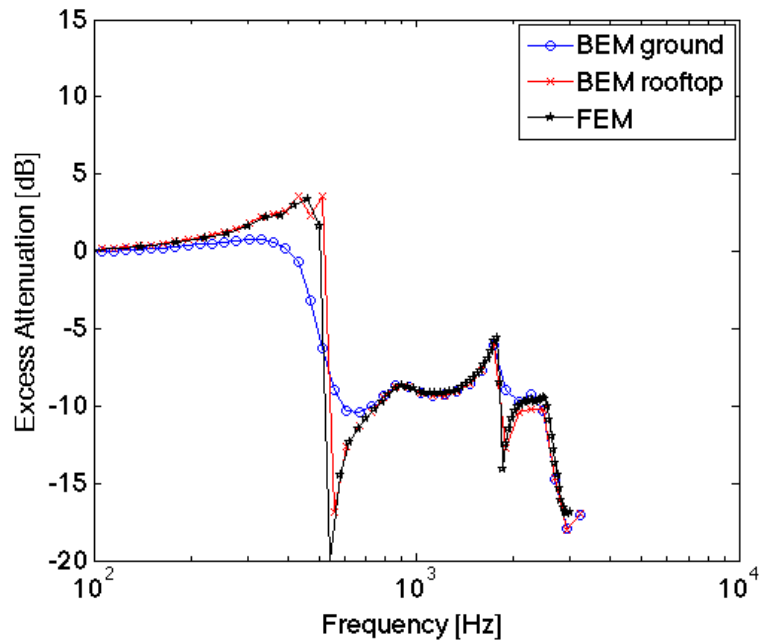


Figure 6.3.: The calculated EA for 5 bosses, calculated for two cases of BEM and one of FEM.

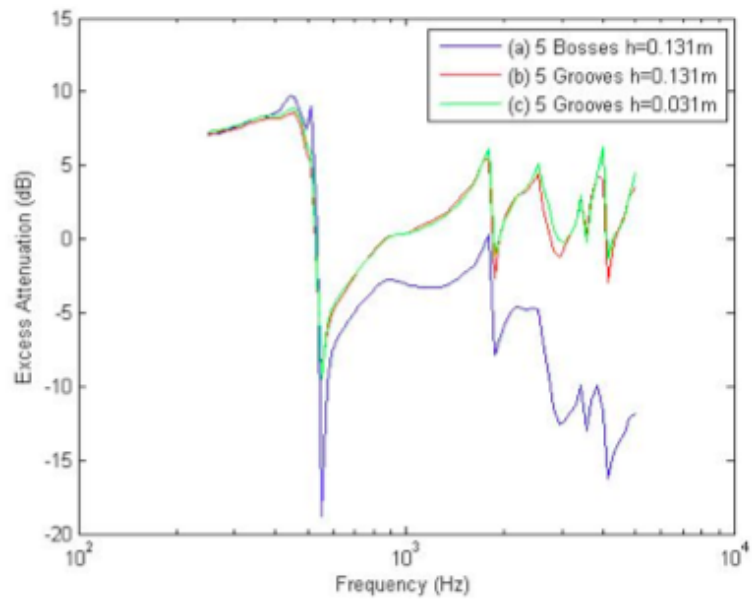


Figure 6.4.: The EA calculated by [20] for 5 bosses. The comparison is made towards the blue curve called a.

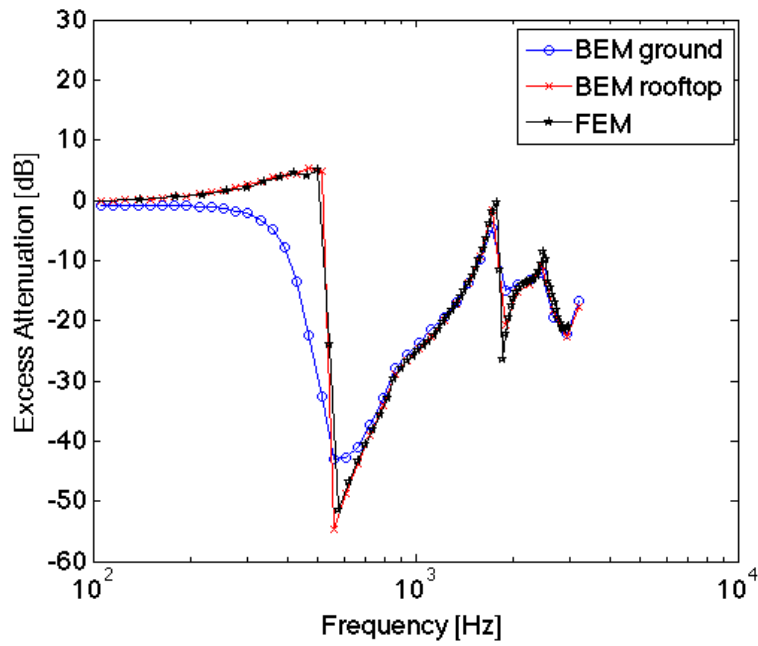


Figure 6.5.: The calculated EA for 15 bosses, calculated for two cases of BEM and one of FEM.

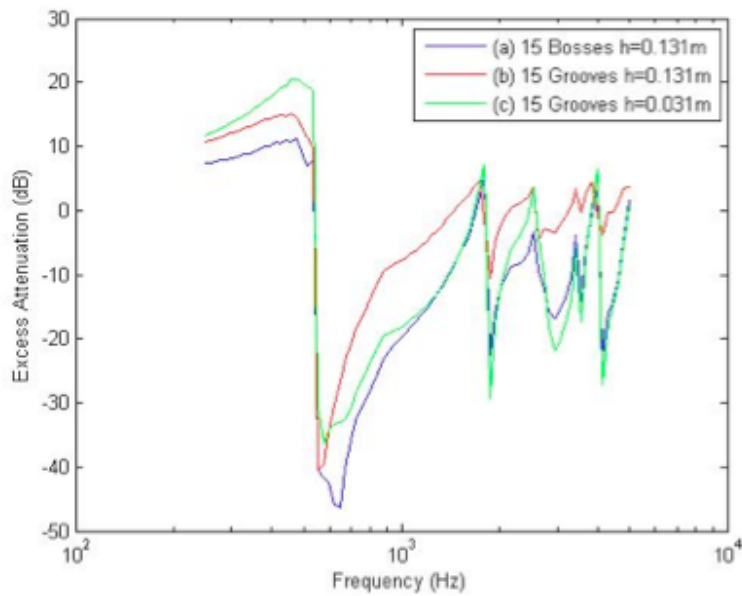


Figure 6.6.: The EA calculated by [20] for 15 bosses. The comparison is made towards the blue curve called a.

The result from the validation shows that the curves are similar enough for the validation to be accepted. The validation also shows that the mirroring method used for the rooftop calculations (when each element is mirrored separately in the x-axis) gives a more exact result.

## 7. Case Studies

In this chapter different case studies examine which parameters influence the performance of the roughness elements and the resulting sound field.

- \* In **case study 1** we examine one single cavity. Here the height  $h$  and the width  $w$  are adjusted.

- \* In **case study 2** we add one more cavity to see how the distance  $dd$  between the cavities influences the result.

- \* In **case study 3** we choose three different cases based on the results from case study 1 and 2 and examine how an increased number of elements affect the result.

The first three situations are studied at ground level. Thereafter the elements are placed on the rooftop of a building, see figure 5.4.

- \* In **case study 4** we choose three different set-ups based on the results from case study 3 and examine what happens when these are placed on the rooftop surrounding a courtyard building.

The result is plotted as the Insertion Loss (IL). The dimensions are all related to our parameter  $q$ , described in chapter 5.2.

### 7.1. Case Study 1: One Cavity: $h$ and $w$ varies

#### 7.1.1. Implementation

In the first case study the influence of the height  $h$  and the width  $w$  of a cavity is under investigation. Only these two parameters will vary. The set up is shown in figure 7.1.

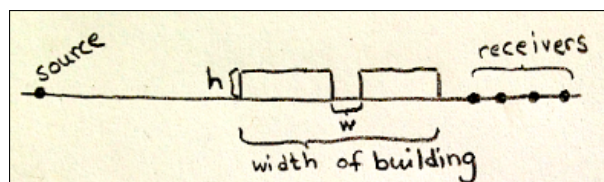


Figure 7.1.: The set up of case study 1

Three different values of  $h$  and three different values of  $w$  are used in the calculations to see what the influence will be if  $q$  increases or decreases. The values used:  $\frac{q}{2}, q, 2q$ . As said in chapter 5.2  $q = 0.85$  m.

### 7.1.2. Result

The results of the Insertion Loss (IL) of case study 1 are shown in figure 7.2 - 7.4. In each plot the height of the element is constant for all three curves while  $w$  is changed. In figure 7.2 the height is set to  $q/2$ , in figure 7.3 the height is set to  $q$  and in figure 7.4 the height is set to  $2q$ .

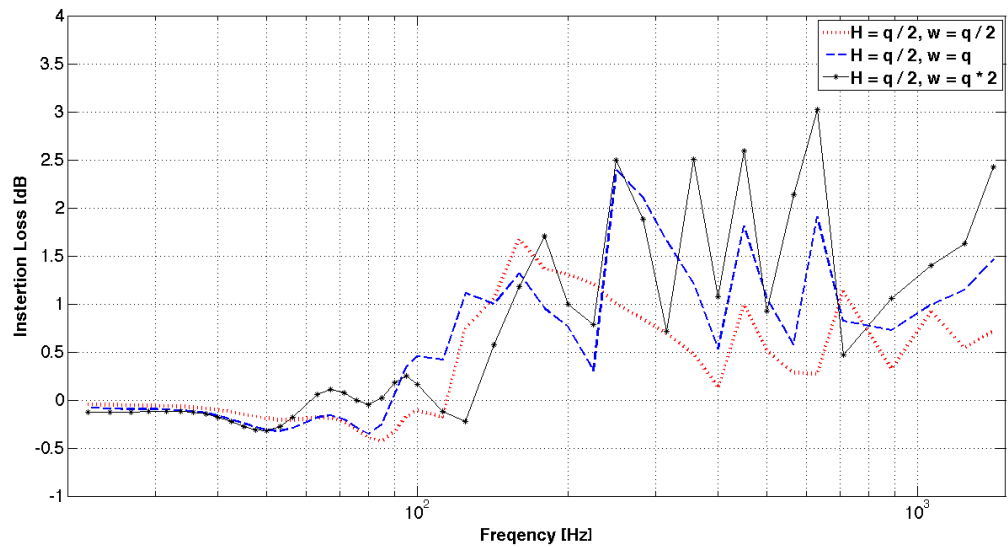


Figure 7.2.: The IL for a fixed height ( $h = \frac{q}{2}$ ) and for a varying width  $w$ .

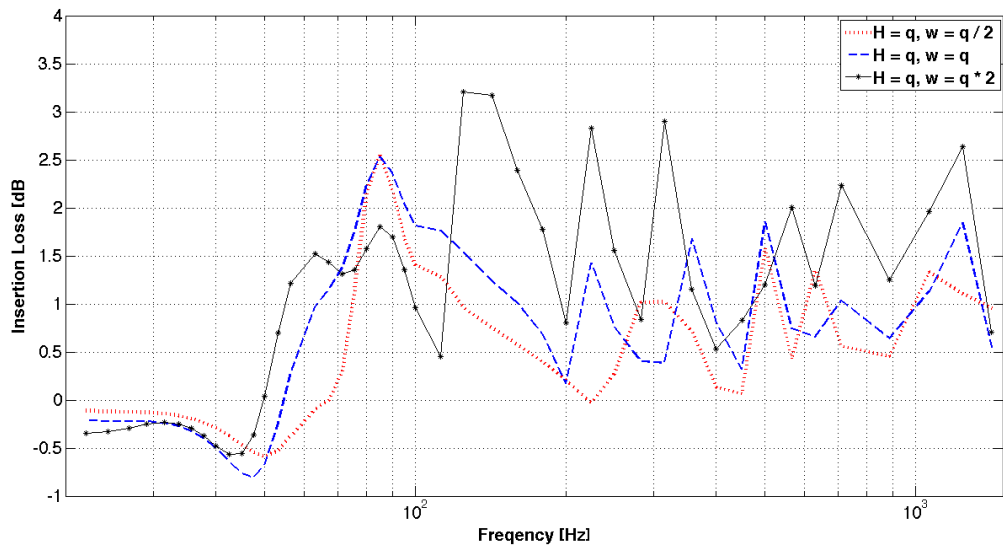


Figure 7.3.: The IL for a fixed height ( $h = q$ ) and for a varying width  $w$ .

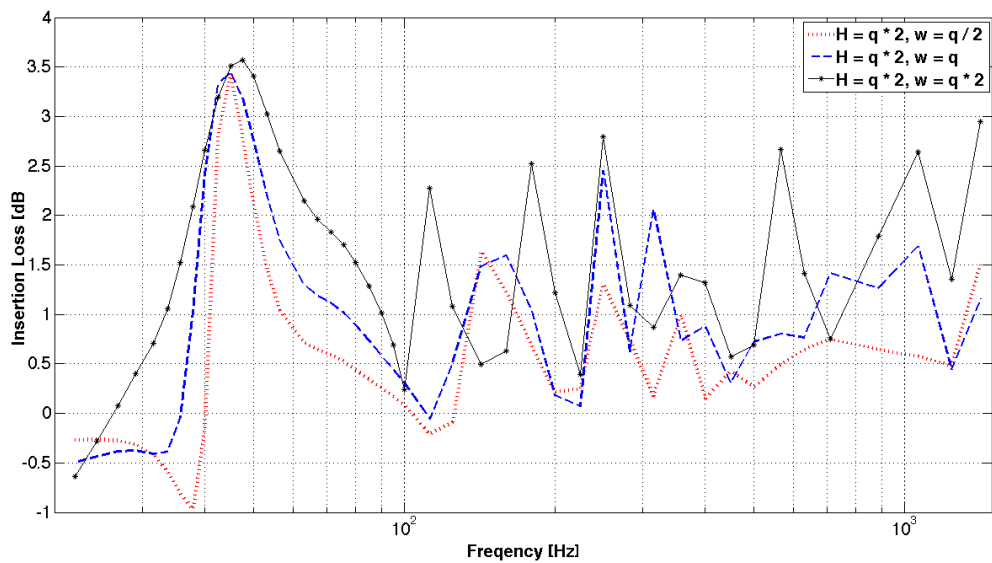


Figure 7.4.: The IL for a fixed height ( $h = q * 2$ ) and for a varying width  $w$ .

### 7.1.3. Analysis

When comparing the results from case study 1 one can see that the height of the first peak of the IL strongly corresponds to the height of the element. When  $h$  increases the first IL-maxima occurs at a lower frequency. One can also see that when  $h$  is bigger

than  $w$  the IL maxima become more narrow. Here the canyon works as a quarter-wave resonator where the target frequency determines the height.

When we have a thin deep cavity the modes will first mainly appear in the direction of the long side (the depth of the cavity). Since this mode will dominate it will be further between the modes making the peak less wide. This can be seen specially in figure 7.4 where the height  $q * 2$  gives a peaks at around 50 Hz.

When  $h$  decreases or when  $w > h$  the IL peak includes a wider frequency range. This is due to that the second IL maximum is enhanced when the centre-to-centre distance increases. This can be seen in figure 7.2 and 7.3.

For the set up of case study 2 the arrangements in figure 7.2 are not of interest since they target a higher frequency range than the one of interest (under 200 Hz). As well will the result in figure 7.4 and the red dotted line in figure 7.3 (where  $h > w$ ) neither be of interest due to the narrow range of targeted frequencies. This is not of interest in this work since we are searching for a solution that works for a broader frequency range.

The most interesting results are found in figure 7.3 where  $h = q$  and  $w = q$  or when  $h = q$  and  $w = 2q$ . Here we target the most of the frequency range that we are interested in. A convergence study is performed to see what happens between these two setups (when  $h = q$  and  $q \leq w \leq 2q$ ), see figure 7.5.

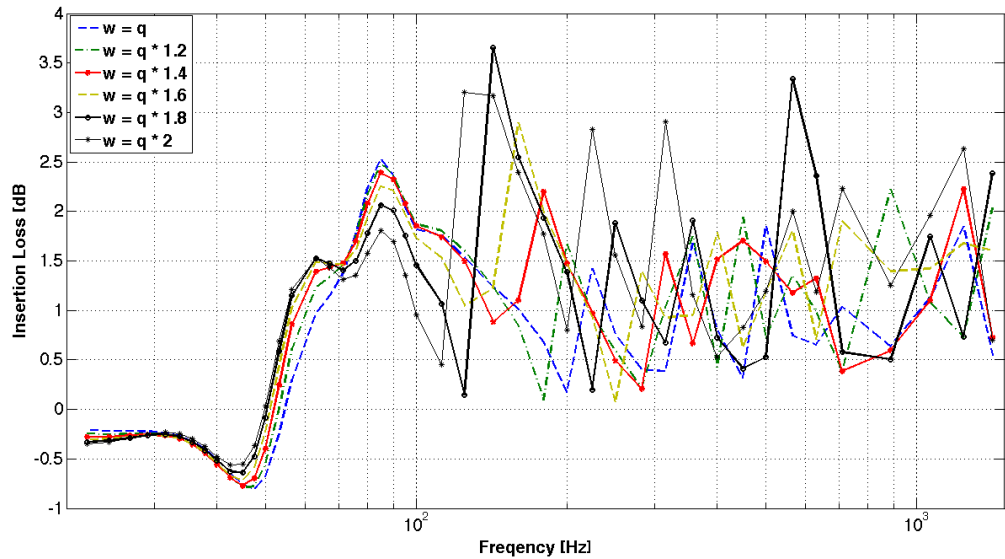


Figure 7.5.: How the IL changes depending on the width of the canyon. The height is constant ( $h = q$ ) while  $w$  vary between  $q$  and  $2 * q$ .

The result shows that as  $w$  increases the second peak as well increases, while the first peak starts to decrease. The first IL peak occurs at around 85 Hz for all six cases studied in figure 7.5.

However the second IL peak occur at different frequencies for the different cases. The wider the spacing of the elements the earlier in frequency the second IL maxima appear. This is most likely due to that another mode shape starts to dominate in the canyon. It might either be in the horizontal direction or in the diagonal direction of the cavity.

Since the goal is to find a configuration which is mostly effective in low frequencies we will now look at the average IL for the cases presented in figure 7.5. The average is taken in the frequency range 31.5 - 200 Hz over four receiver positions, see table 7.1

Table 7.1.: The average IL between 31,5 - 200 Hz for six different widths of the canyon ( $h=q$ ).

Width of canyon [m]:	$q$	$1.2q$	$1.4q$	$1.6q$	$1.8q$	$2q$
Average $IL_{31,5-200\text{Hz}}$ [dB]:	0.73	0.85	0.93	1.01	1.02	1.04

The highest IL is found for a canyon with the width of  $2q$ . However, the biggest increase of the IL due to a wider canyon is found before  $w = 1.6q$ . Thereafter the IL increases more slowly. In the following case study we will therefore look at canyons with both the width of  $1.6q$  and  $2q$  (and with a height of  $q$ ).

## 7.2. Case Study 2: Ground Roughness: 2 Elements with Fixed $h$ , $w$ and Varying $dd$ .

### 7.2.1. Implementation

In case study 2 one more cavity is added to the set up to see how the distance  $dd$  between the canyons influences the result, see the set up in figure 7.6.

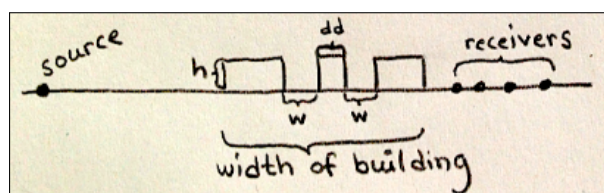


Figure 7.6.: The set up of case study 2.

Due to the result from case study 1 the height of the element is set to  $q$ . Two different widths of the cavities ( $1.6q$  and  $2q$ ) will be examined. The distance between the two



cavities will vary. The following distances will be examined:  $0.1q$ ,  $0.5q$ ,  $1q$ ,  $1.5q$ ,  $2q$ ,  $2.5q$ ,  $3q$ ,  $4q$  where  $q = 0.85$  m.

### 7.2.2. Result

Figure 7.7 and 7.8 show the result of the Insertion Loss (IL) from the calculations of case study 2. In the first figure the width of the cavity is set to  $1.6q$  and in the second figure the width is set to  $2q$ .

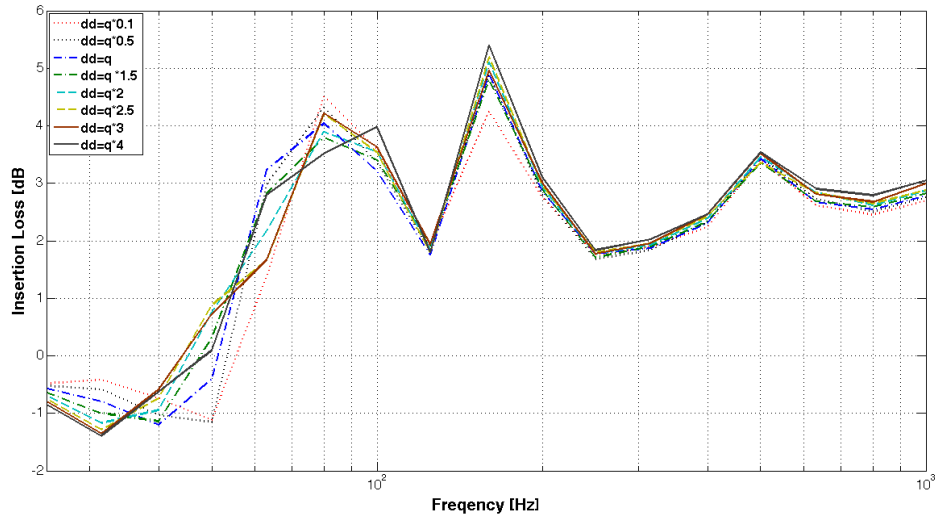


Figure 7.7.: The distance between the two cavities vary while  $h = q$  and  $w = 1.6q$ . The IL is plotted in 1/3 octavebands.

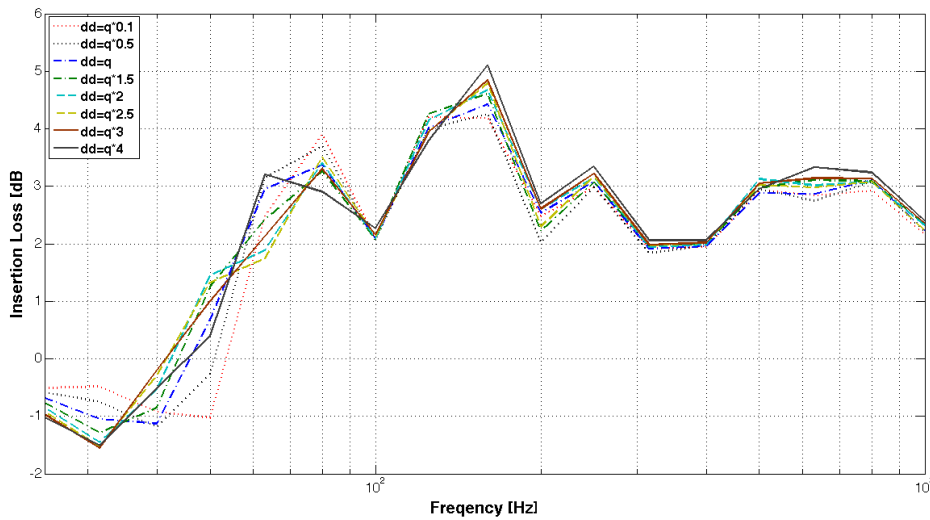


Figure 7.8.: The distance between the two cavities vary while  $h = q$  and  $w = 2q$ . The IL is plotted in 1/3 octavebands.

### 7.2.3. Analysis

Compared to the results from case study 1 one can see that the distance  $dd$  is not as important as a parameter for the final result as the height and width of the cavities. In table 7.2 - 7.3 the average IL between 31.5 - 200 Hz is calculated and presented for the two different widths of the canyons.

Table 7.2.: The average IL for the setup  $h=q$  and  $w=1.6q$ . The distance  $dd$  between the cavities vary.

Distance between cavities [m]:	0.1q	0.5q	q	1.5q	2q	2.5q	3q	4q
Average $IL_{31,5-200Hz}$ [dB]:	1.79	1.93	1.95	1.98	2.02	2.02	2.02	2.07

Table 7.3.: The average IL for the set up  $h=q$  and  $w=2q$ . The distance  $dd$  between the cavities vary.

Distance between cavities [m]:	0.1q	0.5q	q	1.5q	2q	2.5q	3q	4q
Average $IL_{31,5-200Hz}$ [dB]:	1.88	1.89	1.99	2.0	2.03	1.99	2.02	2.04

For case study 3 we would like to have as many canyons as possible. The reason is that previous studies have shown that an increased number of roughness elements has a positive influence on the IL. However since the elements later on will be placed on the top of a roof we will be limited by the width of the building, which is 9.6 m according to chapter 5.3.

We can already see if we look at the results in table 7.1 and compare it to the result in table 7.2 and 7.3 that the average IL is almost twice as big for the case with two cavities compared to one. When the number of elements are increased more energy will be trapped in the cavities.

If we look at the results in table 7.2 we can see that the biggest improvement of the IL happens between  $dd = 0.1q$  and  $dd = 0.5q$ . Therefore case  $dd = 0.5q$  is of interest. In the results in table 7.3 the biggest increase is found between  $dd = 0.5q$  and  $dd = 1q$ .

However, since we also know that the number of elements should be as big as possible we will in the next case study also take a look at the situation where we have as many cavities as possible. This is found by following equations:

$$elements = \frac{w_{Building}}{w} \quad (7.1)$$

If  $w = 1.6q$  and  $w_{Building} = 9.6$ , then the maximum amount of elements will be 7. If  $w = 2q$  the maximum amount of elements will be 5. For these two cases the distance between the cavities  $dd_{min}$  is found by

$$dd_{min} = \frac{w_{Building} - w * (elements - 1)}{elements} \quad (7.2)$$

This will give us two new set ups to investigate:

If  $w = 1.6q$  and  $elements = 7 \implies dd_{min} = 0.15$ .

If  $w = 2q$  and  $elements = 5 \implies dd_{min} = 0.42$

## 7.3. Case Study 3: Ground Roughness: Increasing the Number of Elements

### 7.3.1. Implementation

From case study 2 we found out that distance between the roughness elements does not make a big difference for the result. Therefore based on the result from Case study 1 we will try to fit as many elements as possible within the width of the building. In this section we will look at following cases:

Configuration 1: width of q1.6 with 7 elements,  $dd=0.15$

Configuration 2: width of q1.6 with 6 elements,  $dd=0.41$

Configuration 3: width of q1.6 with 5 elements,  $dd=0.76$

Configuration 4: width of q2 with 5 elements,  $dd=0.42$

Configuration 5: width of q2 with 4 elements,  $dd=0.95$

The distances are calculated by using equation 7.2.

### 7.3.2. Result

The result is divided into two figures where configurations 1, 2 and 3 are plotted in figure 7.9, and configurations 4 and 5 are plotted in figure 7.10.

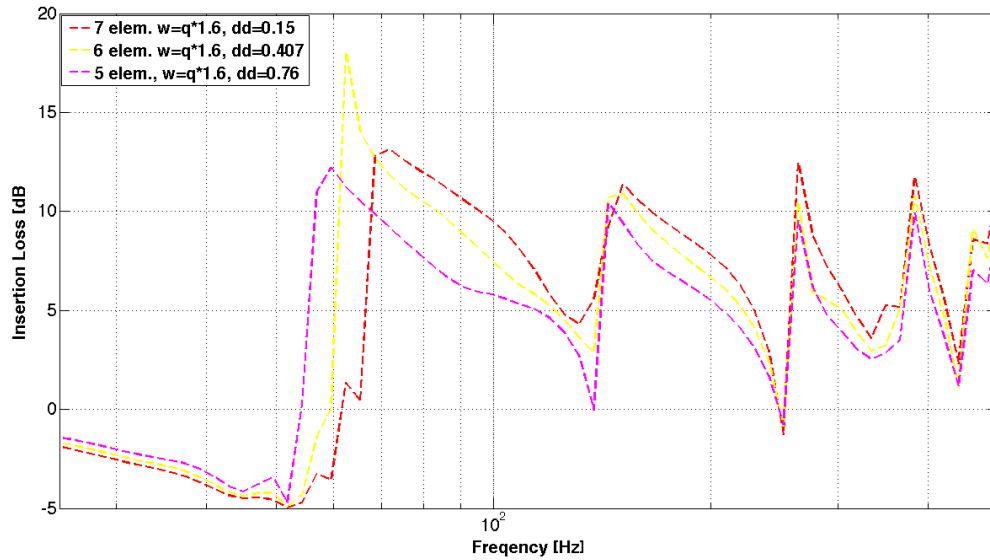


Figure 7.9.: The IL for three different set ups.  $h = q$  and  $w = 1.6q$

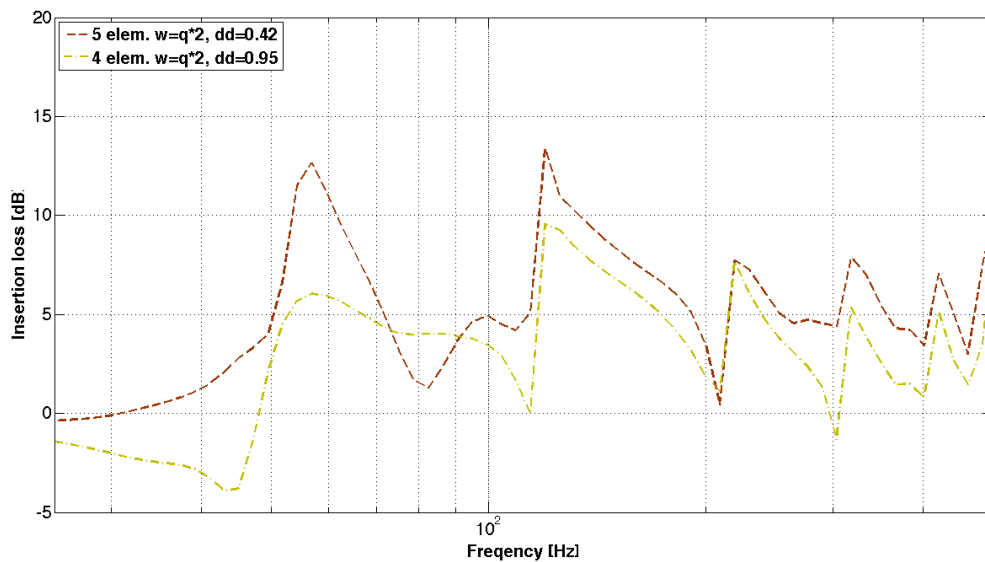


Figure 7.10.: The IL for two different set ups.  $h = q$  and  $w = 2q$

### 7.3.3. Analysis

In the result in figure 7.9 and 7.10 we can see that there is an increase in the Insertion Loss (IL) when the number of cavities are increased. Apart from the first peak, the shape of the curves acts similarly. We will one more time look at the average IL between 31.5-200 Hz. It is shown in table 7.4.

Table 7.4.: The averaged IL for 5 different set ups in case study 3.

Configuration:	1	2	3	4	5
Average $IL_{31,5-200\text{Hz}}$ [dB]:	3.6	3.4	3.6	4.7	2.4

The result shows that configuration 4 gives the best result (seen in figure 7.10 as the red curve). This is most likely due to that there is no dip in the curve under 60 Hz as for the other cases.

## 7.4. Case study 4: Adding Roughness Elements to the Rooftop.

### 7.4.1. Implementation

In this case study the configurations which have been identified through case study 1-3 will be placed on the rooftop of a courtyard building. The set up of the courtyard is taken from [33] and shown in figure 7.11 (more information is given in chapter 5.3).

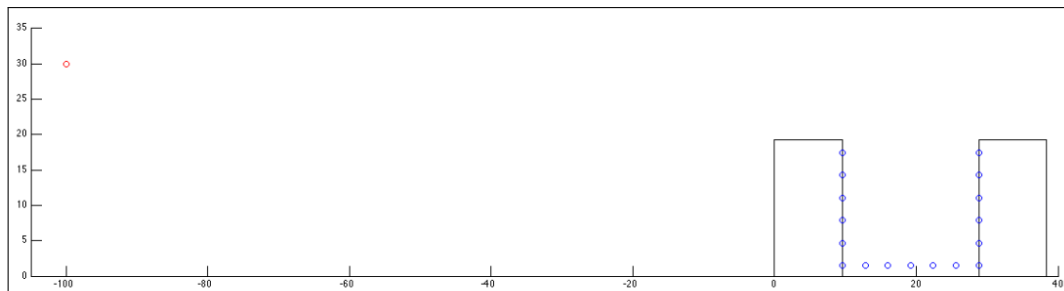


Figure 7.11.: Set up of the courtyard where the red ring represents the source and the blue rings represents the receiver positions.

The source represents the exhaust pipe of a cruise ship at a distance of 100 m from the first building. The height of the source is 30 m. The courtyard consists of two six storey high buildings with a total height of 19.2 m. The result will be calculated at three different zones in the courtyard: the exposed facade, at ear height (1.5 m), and at the shadowed side of the courtyard, see figure 7.12

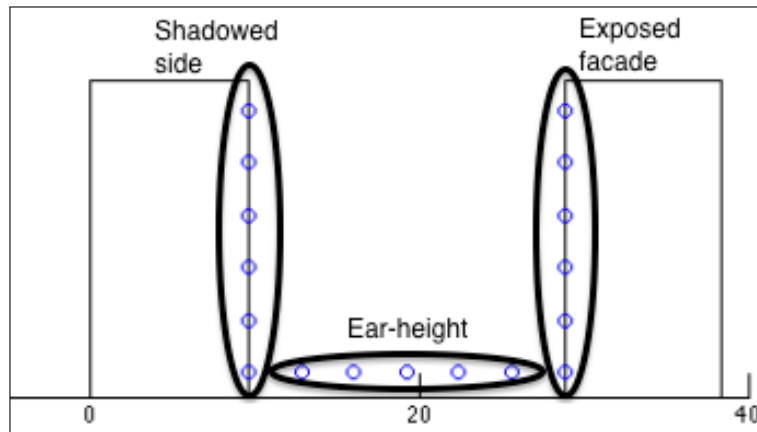
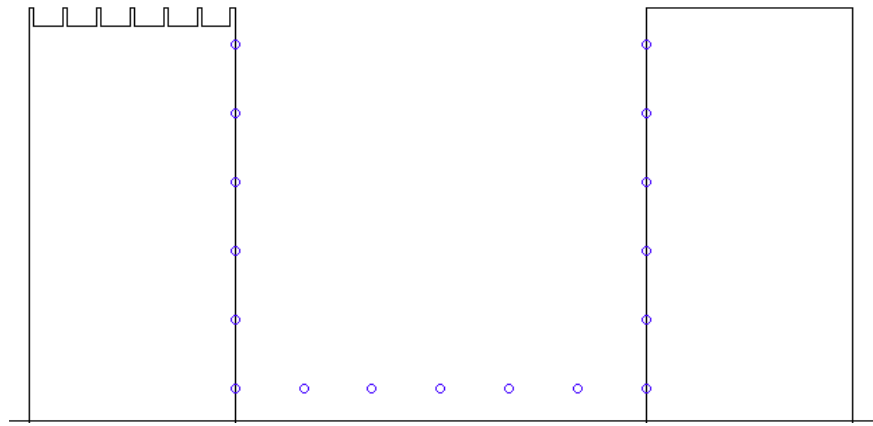
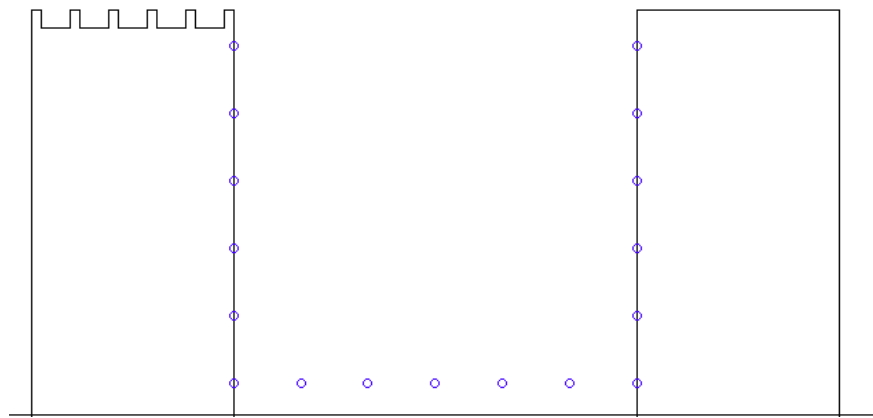


Figure 7.12.: The three different examined zones in the courtyard.

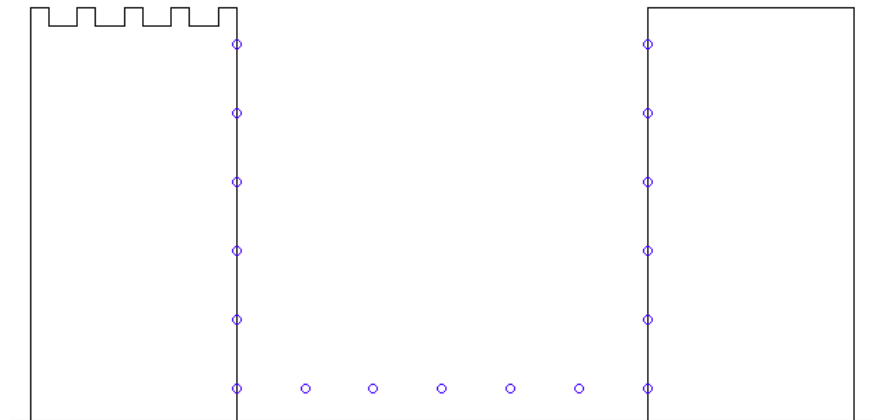
From the previous studies (Case study 3) we found that the configuration 4, with a width of  $2q$  and 5 elements, gave the best result for the IL between 31.5-200 Hz. However we are also interested in placing as many roughness elements as possible at the rooftop. Therefore we will also examine configurations 1 and 2 from Case study 3. The three configurations will be called Case 1, 2 and 3 and are presented in figure 7.13.



(a) Set up for Case 1.



(b) Set up for Case 2.



(c) Set up for Case 3.

Figure 7.13.: Three different configurations of roughness elements at a rooftop. Receiver positions are marked with blue dots.

### 7.4.2. Result

The IL has been calculated for all three configurations. In the following figures the IL at each receiver position has been compared to the Sound Pressure Level (SPL) from the source, see section 5.1, at a distance of 100 m. In figure 7.14 the result at the 6 first positions at the shadowed side of the first building are plotted, in figure 7.15 the result at the 5 position at ear height in the courtyard are plotted and in figure 7.16 the result at the 6 last positions at the exposed facade of the second building are plotted.

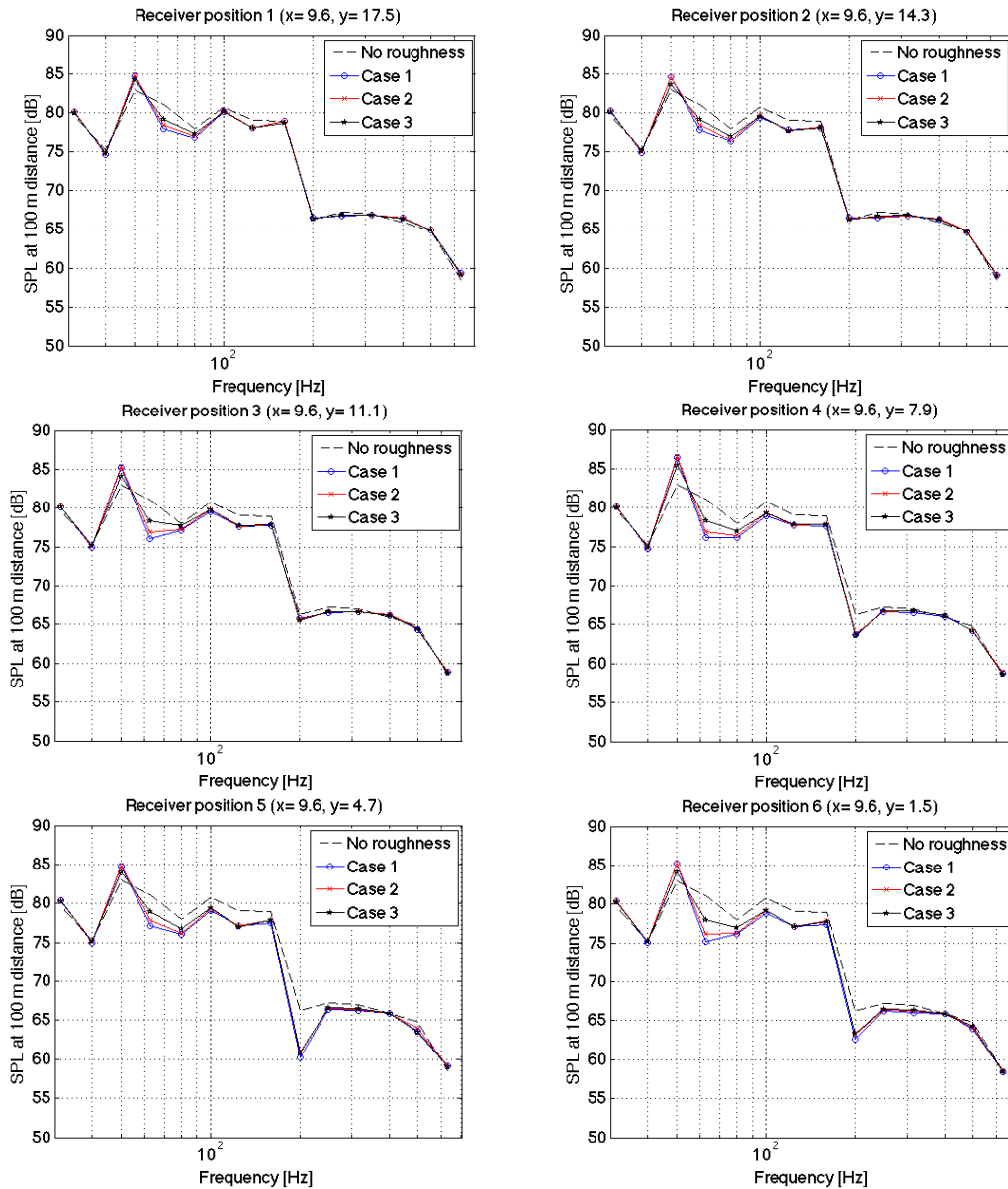


Figure 7.14.: The SPL at the shadowed side.



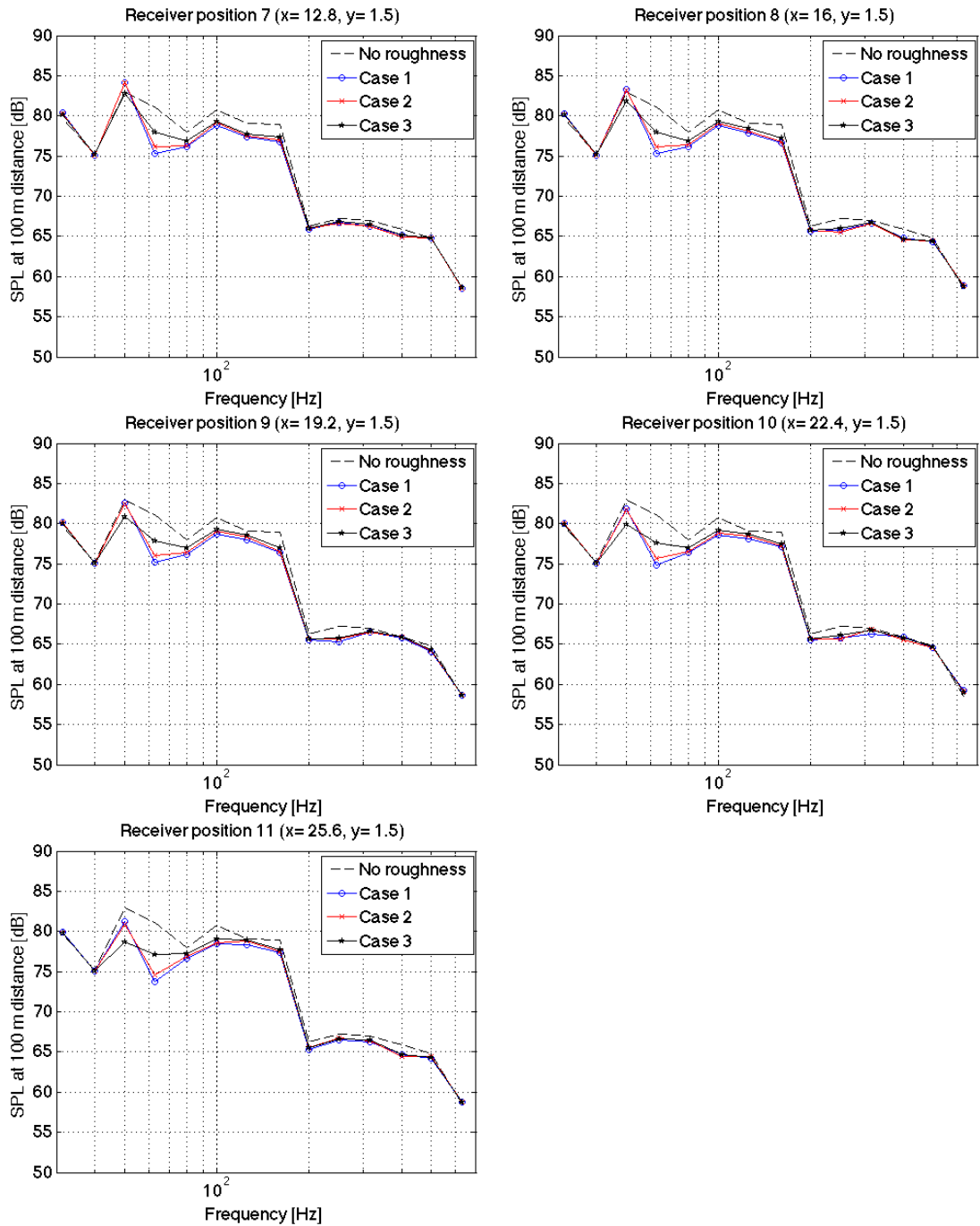


Figure 7.15.: The SPL at ear height (1.5 m above ground).

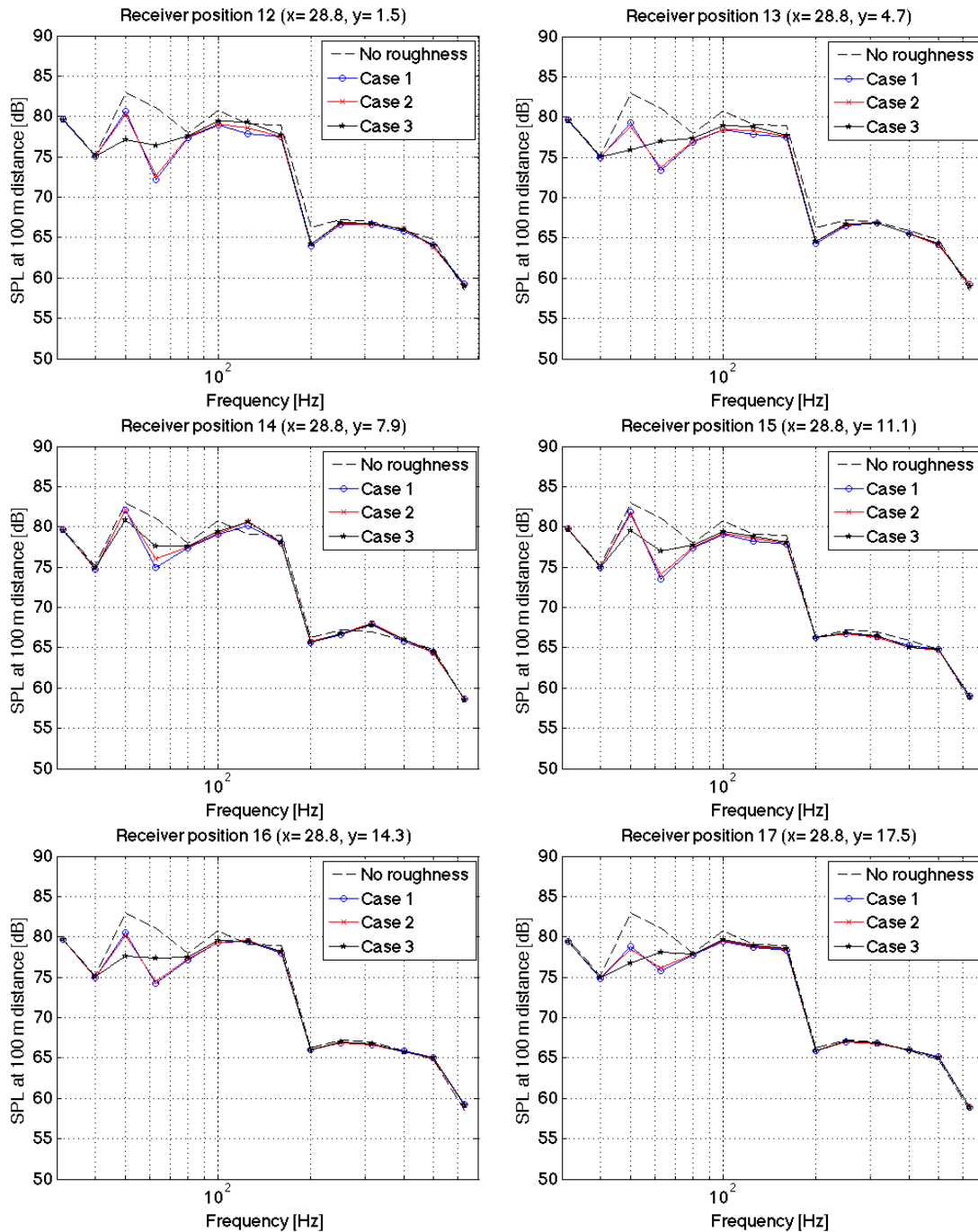


Figure 7.16.: The SPL at the exposed facade.

The source spectrum is the same for all plots.

### 7.4.3. Analysis

As we can see from the graphs Case 1 and 2 give a similar result at all receiver positions, while there is a small difference in the result for Case 3. As we know from chapter 7.2 the distance between the cavities plays a small role. This statement is then also confirmed here.

That Case 1 shows a slightly higher IL than Case 2 is due to that Case 1 consists of a higher number of roughness elements than both Case 2 and Case 3.

There is a peak in the insertion loss at 63 Hz, This peak occurs for all three cases at all receiver positions. Most likely it is due to the depth of the roughness elements since the depth is the same for all three configurations. However to be sure of this it we would need more investigations with different depth of the cavities.

There is a positive IL from 40 - 200 Hz at all positions.

## 8. Summary

For these kinds of studies, where outdoor noise propagation is modelled, the Boundary Element Method (BEM) has more advantages than the Finite Element Method (FEM). The main advantage with BEM is that only the boundary of the scattering object needs to be discretized and not the whole domain, as for the FEM.

Benefits of roughness elements compared to e.g. noise barriers is that they do not have the same visual impact on the environment as barriers. The roughness elements can be tuned to abate low-frequent noise without needing to block the line of sight between the source and the receiver.

The results from the case studies show that to affect a wider range of frequencies the **width** of the cavity should be bigger than the height

$$w > h \quad (8.1)$$

However the **height** decides which frequency region will be affected in the first place.

The **distance** between the canyons turned out to be of small importance.

If the **number of roughness elements** are increased more energy will be trapped inside the cavities.

Form the result of case study 4 we can see that elements of a height of 0.85 m and with a cavity width of 1.36 m give a reduction in the frequency range 40-200 Hz with a peak insertion loss of 8 dB in the 63 Hz 1/3 octave band.

The final result showed that it is possible to decrease low frequent noise by using roughness elements.



## References

- [1] Ang W.T.: *A Beginner's Course in Boundary Element Methods*, Universal Publishers, Boca Raton, USA, (2007)
- [2] O'Neil, M., Greengard, L. and Pataki, A.: *On the efficient representation of the half-space impedance Greens function for the Helmholtz equation*, *Wave Motion*, Vol. 51, No. 1, Elsevier (2014), pp. 1-13.
- [3] Kirkup, S. and Yazdani, J.: *A Gentle Introduction to the Boundary Element Method in Matlab/Freemat*, Report AR-08-14, East Lancashire Institute of Higher Education, Blackburn, UK, <http://www.boundary-element-method.com/AR0814BEM.pdf> (last visited 2015/04/06)
- [4] Mechel, F. P. and Ochmann, M.: *Analytical and Numerical Methods in Acoustics*, Springer-Verlag, Berlin Heidelberg, (2004)
- [5] Thorsson, P.: *Optimisation of Low-Height Sound Barriers*, Master thesis, Department of Applied Acoustics, Chalmers University of Technology, Göteborg, (1998)
- [6] Park, J. M. and Eversman, W.: *A boundary element method for propagation over absorbing boundaries*, *Journal of Sound and Vibration*, Vol. 175, No. 2, Elsevier (1994), pp. 197-218.
- [7] Dean G. Duffy: *Greens Functions with Applications*, Chapman and Hall/CRC, London, (2001)
- [8] Gao, H., Matsumoto, T., Takahashi, T. and Isakari, H.: *Analysis of acoustic transmission for one directional periodic bounded structure in 2D by BEM*, *Transactions of JASCOME* Vol. 12, No. 12-121212, (Dec. 2012)
- [9] Brick, H.: *Application of the Boundary Element Method for combustion noise and half-space problems*, PhD thesis, Department of Applied Acoustics, Chalmers University of Technology, Göteborg, (2009)
- [10] Schneck, H.A. *Improved integral formulation for acoustic radiation problems* *Journal of the Acoustic Society of America* (1968)
- [11] Loyd's Register *ODSNoise from ships in ports Possibilities for noise reduction*, Environmental Project No. 1330, Miljprojekt, Danish Ministry of the Environment, Copenhagen (2010) <http://mst.dk/media/mst/66165/978-87-92668-35-6.pdf> (last visited 2015/04/07)

- [12] *Stadens ljud Seminarium i Göteborg 28 mars 2012* presented by Rudeberg, G. from Stockholm Hamnar,(2012) [http://hplus.helsingborg.se/ImageVaultFiles/id27171/cf\\_2/Stockholms\\_hamnar.PDF](http://hplus.helsingborg.se/ImageVaultFiles/id27171/cf_2/Stockholms_hamnar.PDF) (last visited 2015/04/07) (Swedish source)
- [13] Badino, A., Borelli, D., Gaggero T., Rizzuto, E. and Schenone, C.: *Analysis of airborne noise emitted from ships*, Journal of Sound and Vibration Sustainable Maritime Transportation and Exploitation of Sea Resources, Taylor & Francis Group, London (2012).
- [14] Biot, M. and Moro, L.: *Advances in Marine Structure (Methods and criteria to manage airborne outdoor ship noise)*, Taylor & Francis Group, London (2011), ISBN 978-0-415-67771-4
- [15] *BULLER en utmaning för hamnars framtida utveckling* Resultat från PENTA-projektet: presented by Mustonen, M. from TFK - TransportForsK at VTI TransporForum, (2013) (Swedish source)
- [16] Delente, M. *WP 5: GREEN LABEL PROPOSAL - Subtask 5.2: Noise and Vibration label proposal*, SILNV (Ships oriented Innovative soLutions to rEduce Noise and Vibrations),FP7 - Collaborative Project No. 234182 (2012) [http://www.silenv.eu/green\\_label/D5.2\\_green\\_label\\_rev\\_2.pdf](http://www.silenv.eu/green_label/D5.2_green_label_rev_2.pdf) (last visited 2016/02/15)
- [17] Badino, A., Borelli, D., Gaggero T., Rizzuto, E. and Schenone, C.: *Control of Airborne Noise Emissions from Ships*. MARNNAV 2012, International Conference on Advances and Challenges in Marine Noise and Vibration, Glasgow, United Kingdom, (2012)
- [18] Witte, J.: *Noise from moored ships*, Internoise ,Lisbon, Portugal, 2010 [http://dgm.nl/uploads/files/Internoise\\_2010\\_Rob\\_Witte\\_Noise\\_from\\_moored\\_ships.pdf](http://dgm.nl/uploads/files/Internoise_2010_Rob_Witte_Noise_from_moored_ships.pdf) (last visited 2016/02/15)
- [19] Hallin, A., Halling, C., Lindqvist, M. and Akerlof, L.: *Trafikbuller och planering IV* Kaigan, Sundbyberg, Sweden 2012. ISBN: 978-91-85125-47-0
- [20] Attenborough, K., Taherzadeh, S., Bashir, I. and Hill, T.: *Work Package 4 - Acoustical effects of rough surfaces* HOSANNA Collaborative Project N. 234306, (2011)
- [21] van der Heijden, L. A. M. and Martens, M. J. M.: *Traffic Noise Reduction by Means of Surface Wave Exclusion Above Parallel Grooves in th Roadside*. Applied Acoustics 15 (1982) p.329-339
- [22] Taherzadeh, S., Hill, T., Taherzadeh, S., Attenborough, K. and Hornikx, M. *Reduction of surface transport noise by ground roughness*. Applied Acoustics 83 (2014) p. 115

- [23] Bougdah, H., Ekici, I. and Kang, J.: *A laboratory investigation of noise reduction by riblike structures on the ground*. J. Acoust. Soc. Am. 120 (6), December 2006
- [24] Bashir, I., Taherzadeh, S., Hill, T.J. and Attenborough, K. *Diffraction-assisted rough ground effects*. Proceedings of the Acoustics 2012 Nantes Conference, 23-27 April 2012, Nantes, France
- [25] Crocker, M. J.: *Handbook of Noise and vibration control*. John Wiley & Sons, Inc (2007) ISBN: 978-0-471-39599-7
- [26] Faure, O., Gauvreau, B., Junker, F. and Lafon, P. *Experimental validation of the modelling of surface roughness effects by an effective impedance*. Internoise, Melbourne, Australia, 2014, [http://www.acoustics.asn.au/conference\\_proceedings/INTERNOISE2014/papers/p214.pdf](http://www.acoustics.asn.au/conference_proceedings/INTERNOISE2014/papers/p214.pdf) (last visited 2016/02/15)
- [27] Attenborough, K., Taherzadeh, S., Bashir, I. and Hill, T.: *Work Package 4 - The acoustical performance of parallel wall systems* HOSANNA Collaborative Project N. 234306, (2012)
- [28] Tolstoy, I.: *Smoothed boundary conditions, coherent low-frequency scatter, and boundary modes*. J. Acoust. Soc. Am. 75 (1), January 1984
- [29] Van Renterghem, T., Forssen, J., Attenborough, K., Jean, P., Defrance, J., Hornikx, M. and Kang, J.: *Using natural means to reduce surface transport noise during propagation outdoors*. Applied Acoustics 92 (2015) pp. 86101
- [30] Attenborough, K., Li, K. M. and Horoshenkov, K. *Predicting Outdoor Sound* CRC Press Taylor & Francis Group, London, (2007) ISBN 9780419235101
- [31] Ingard, U. *On the theory and design of acoustic resonators*. The journal of the Acoustical Society of America, vol. 25, num. 6, (1953) pp. 10371327
- [32] Boulanger, P., Attenborough, K., Taherzadeh, S., Waters-Fuller, T. and Li, K. M. *Ground effect over hard rough surfaces*. J. Acoust. Soc. Am., Vol. 104, No. 3, (1998) pp.1474-1482
- [33] Hornikx, M., Smyrnova, Y., van Renterghem, T., Cheal, C. and Kang, J.: *Work Package 5 - Green Buildings* HOSANNA Collaborative Project N. 234306, (2012)
- [34] *Folkhalsomyndighetens allmänna rad om lagfrekvens buller* FoHMFS 2014:13, (2014) (Swedish source)





# A. Matlab-code

## Part 1,2,3

### BEM2GroundelementsCase1.m

```
% BEM Case 1
% Code made by Anna Novak and Bart van der Aa

clc
clear all
close all

DateNumber=('06-Jan-2015');

c0 = 340;%Speed of sound
NPPW = 20;% Spatial sampling (points per wavelength)
N_leg = 10;% Order of Gauss-Legendre quadrature
N_Chief = 8;% Number of CHIEF points per element

%Frequency vector:
a=log10(22.4); b=log10(1120);
f_vec=logspace(a,b,(17*5));
f_start=f_vec(1);
f_max=f_vec(end);

Nf = length(f_vec);
k_vec = 2*pi*f_vec/c0;

% Receiver positions, the first 4 are at ground level.
zr=[0 0 0 0 0.2 0.4 0.6 0.8 1 1.2 1.4 1.6 1.8 2 2.5 3 0 0.2 0.4 0.6 0.8
1 1.2 1.4 1.6 1.8 2 2.5 3];
xr = zeros(1,length(zr))-3; %The first 16 positions are adjusted later
Nr = numel(zr); % Number of receiver locations

% Source positions
xs = -50; % x-coordinate source
hs = 0; % z-coordinate source

%Pressures
Pd = zeros(Nf,Nr); % Direct pressure
Pdr = zeros(Nf,Nr); % Total pressure, without barrier
Ptot = zeros(Nf,Nr); % Total pressure, with barrier

W_building = 9.6;
```

```

%%%%%%%%%%%%%%%%%%%%%%%%%%%%%%%%%%%%%%%%%%%%%%%%%%%%%%%%%%%%%%%%%%%%%%%%
%This coming part changes for Case Study 2 and 3.
%%%%%%%%%%%%%%%%%%%%%%%%%%%%%%%%%%%%%%%%%%%%%%%%%%%%%%%%%%%%%%%%%%%%%%%%

% The roughness elements
elements_vec = 2; %In Case study 2
lam=0.85; %Called q in the report

% For the first calculations
lamHeight=[lam/2 lam lam*2];
lamWidth=[lam/2 lam lam*2];

% % For the convergence study
% lamheight=[lam];
% lamwidth=[lam lam*1.2 lam*1.4 lam*1.6 lam*1.8 lam*2];

for aa=1:length(lamHeight)
    lamH=lamHeight(aa)

for bb=1:length(lamWidth)
    lamW=lamWidth(bb)
    canyon=W_building/2-lamW/2;

for ii=1:elements_vec(end)
eval(['xy_vec_' num2str(ii) '=[canyon*' num2str(ii-1) '+lamW*'
num2str(ii-1) ' canyon*' num2str(ii-1) '+lamW*' num2str(ii-1) '
canyon*' num2str(ii) '+lamW*' num2str(ii-1) ' canyon*' num2str(ii)
'+lamW*' num2str(ii-1) '; 0 lamH lamH 0];']);

eval(['xy_vec_chief_X' num2str(ii) '=[canyon/3+(lamW+canyon)*'
num2str(ii-1) ' canyon/4+(lamW+canyon)*' num2str(ii-1) '
canyon/5+(lamW+canyon)*' num2str(ii-1) ' canyon/2+0.5+(lamW+canyon)*'
num2str(ii-1) ' canyon/2+0.3+(lamW+canyon)*' num2str(ii-1) '
canyon/4+0.4+(lamW+canyon)*' num2str(ii-1) ' canyon/2+0.35+(lamW+canyon)*'
num2str(ii-1) ' canyon/6+(lamW+canyon)*' num2str(ii-1) '];']);
xy_vec_chief_Y=[lamH*0.06 lamH*0.25 lamH*(-0.402) lamH*(-0.162) lamH*0.981
lamH*(-0.89) lamH*0.285 lamH*(-0.5)];
eval(['xy_vec_chief_' num2str(ii) '=[xy_vec_chief_X' num2str(ii) '
xy_vec_chief_Y];'])
end

for jj=1:length(elements_vec)

    element= elements_vec(jj);%Number of elements, in this case 2

    VEC_last=0;

    %Creating the elements
    for mm=1:element
        eval(['xy_vec=xy_vec_' num2str(mm) '];']);
        eval(['xy_chief=xy_vec_chief_' num2str(mm) '];']);
    end
end

```

```

    % The nodes are drawn in following function
    [xyVEC DL n_Hat VECC]=nodes_Roughness_ground(c0, f_vec, NPPW,
xy_vec);

    %To make space in the vectors
    VEC=VEC_last+1:(VEC_last+VECC);

    %Connect the elements
    xy(VEC,1)=xyVEC(:,1);
    xy(VEC,2)=xyVEC(:,2);
    n_hat(VEC,1)=n_Hat(:,1);
    n_hat(VEC,2)=n_Hat(:,2);
    dl(VEC,1)=DL(:,1);

    % Make vector of Chief-points
    xy_chief=xy_chief';
    XY_CHIEF(N_Chief*(mm-1)+1:N_Chief*mm,:)=xy_chief;

    VEC_last=VEC(end);
end

N_CHIEF=length(XY_CHIEF);
N2=length(xy);

% Adjusting the receiver positions
xr(1)=max(xy(:,1))+3;
xr(2)=max(xy(:,1))+3.5;
xr(3)=max(xy(:,1))+4;
xr(4)=max(xy(:,1))+2.1;
xr(5:16)=max(xy(:,1))+3; % Elevated sources

% Main loop
for nf = 1:Nf

    f_vec(nf)
    k = k_vec(nf);

    % N-th order Gauss-Legendre quadrature, with position terms R_leg,
and weight
    % terms W_leg
    N_leg=10;
    R_leg=[-0.9739 -0.8651 -0.6794 -0.4334 -0.1489 0.1489 0.4334 0.6794
0.8651 0.9739]';
    W_leg=[0.0667 0.1495 0.2191 0.2693 0.2955 0.2955 0.2693 0.2191 0.1495
0.0667];

    % Each element is described as 10 points from -dl/2 to dl/2. The node
% is positioned at the centre of ech surface element
    xy_leg=zeros(N2,2,N_leg);
    for n=1:N2
        xy_leg(n,1,:)=xy(n,1)+.5*dl(n)*R_leg*n_hat(n,2);
    end
end

```

```

        xy_leg(n,2,:)=xy(n,2)+.5*dl(n)*R_leg*n_hat(n,1);
end

% Exciting field:
xy0 = [xs hs];
xy0Mat(1,:) = xy0;
Rd = sqrt(sum((xy0(ones(N2),1,:)-xy(1:N2,:)).^2,2));

xy0 = [xs -hs];
xy0Mat(2,:) = xy0;
Rr = sqrt(sum((xy0(ones(N2),1,:)-xy(1:N2,:)).^2,2));

xy0 = xy0Mat(1,:);
Rd_chief=sqrt(sum((xy0(ones(N_CHIEF,1),:)-XY_CHIEF(1:N_CHIEF,:)).^2,2));
xy0 = xy0Mat(2,:);
Rr_chief=sqrt(sum((xy0(ones(N_CHIEF,1),:)-XY_CHIEF(1:N_CHIEF,:)).^2,2));

N_tot=N2;
beta=zeros(N2,1); % The admittance is set to zero

% The "transfer matrix"
A = zeros(N2,N2);

%The calculations are done for each surface element
for m = 1:N2
    xy0=xy(m,:);

    Rtmp = reshape(sqrt((xy0(1)-xy_leg(:,1,:)).^2+(xy0(2)-xy_leg(:,2,:)).^2),N2,N_leg);

    r_hat_leg=zeros(N2,N_leg,2);
    r_hat_leg(:,:,1) = reshape(xy0(1)-xy_leg(:,1,:),N2,N_leg)./Rtmp;
    r_hat_leg(:,:,2) = reshape(xy0(2)-xy_leg(:,2,:),N2,N_leg)./Rtmp;

    n_hat_leg=zeros(N2,N_leg,2);
    for n=1:N_leg
        n_hat_leg(:,n,:)=n_hat;
    end

    % Pressure green's function:
    G_leg = (1i/4)*besselh(0,1,k.*Rtmp);

    % Velocity green's function:
    DRG_leg = -((1i*k)/4)*besselh(1,1,k.*Rtmp);

    dim = 3; % In which matrix dimension to take dot product
    dotprod_leg=dot(n_hat_leg,r_hat_leg,dim);
    DnGv_leg=DRG_leg.*dotprod_leg; % projection on normal

    Gji = sum(G_leg.*W_leg(ones(N2,1),:),2)/2;

```

```

DnGvj_i = sum(DnGv_leg.*W_leg(ones(N2,1),:),2)/2;

gamma_ji = ((1i*k*beta(1:N2).*Gji(1:N2)+DnGvj_i(1:N2)).*dl(1:N2))
.'; % -m bec. own--own not included in vector % Later, make more
precise with integrals

A(m,:) = gamma_ji;
A(m,m) = A(m,m)+(1/2); %1/2 due to the SHIE
end

%The procedure is repeated for the chief-points
for mc = 1:N_CHIEF;
    xy0 = XY_CHIEF(mc,:); % xy0 is temporary CHIEF point

    Rtmp = reshape(sqrt((xy0(1)-xy_leg(:,1,:)).^2+(xy0(2)-
xy_leg(:,2,:)).^2),N2,N_leg);

    r_hat_leg=zeros(N2,N_leg,2);
    r_hat_leg(:,:,1)=reshape(xy0(1)-xy_leg(:,1,:),N2,N_leg)./Rtmp;
    r_hat_leg(:,:,2)=reshape(xy0(2)-xy_leg(:,2,:),N2,N_leg)./Rtmp;

    n_hat_leg=zeros(N2,N_leg,2);
    for n=1:N_leg
        n_hat_leg(:,n,:)=n_hat;
    end

    % Pressure green's function:
    G_leg = (1i/4)*besselh(0,1,k.*Rtmp);

    % Velocity green's function:
    DRG_leg = -(1i*k)/4*besselh(1,1,k.*Rtmp);
    dim = 3; % in which matrix dimension to take dot product
    dotprod_leg=dot(n_hat_leg,r_hat_leg,dim);
    DnGv_leg=DRG_leg.*dotprod_leg; % projection on normal

    Gji = sum(G_leg.*W_leg(ones(N2,1),:),2)/2;
    DnGvj_i = sum(DnGv_leg.*W_leg(ones(N2,1),:),2)/2;

    gamma_ji = ((1i*k*beta(1:N2).*Gji(1:N2)+DnGvj_i(1:N2)).
.*dl(1:N2)).'; % -m bec. own--own not included in vector

    A(N2+mc,:)=gamma_ji;
end

% SOLVE:
%-----
Pinc = zeros(N2+N_CHIEF,1);
Pinc(1:N2) = (1i/4)*besselh(0,1,k.*Rd) + (1i/4)*besselh(0,1,k.*Rr);
Pinc(N2+1:end) = (1i/4)*besselh(0,1,k.*Rd_chief) + (1i/4)*
besselh(0,1,k.*Rr_chief);
P=A\Pinc;
%-----

```

```

% Loop through the receiver locations:
for ii = 1:Nr

    R0d = sqrt(sum(([xs hs]-[xr(ii) zr(ii)].^2)); % Direct path
    R0r = sqrt(sum(([xs -hs]-[xr(ii) zr(ii)].^2)); % Reflected path

    Pd(nf,ii) = (1i/4)*besselh(0,1,k.*R0d); % Direct pressure
    Pdr(nf,ii) = (1i/4)*besselh(0,1,k.*R0d) + (1i/4)*besselh(0,1,k.
    *R0r);
    %Direct + groundreflected pressure

    xy0 = [xr(ii) zr(ii)];
    R = sqrt(sum((xy0(ones(N2,1),:)-xy).^2,2));

    % Pressure sources:
    Gjrec = (1i/4)*besselh(0,1,k.*R);

    % Velocity sources:
    r_hat = (xy0(ones(N2,1),:)-xy)./R(:,ones(1,2));
    dim = 2;
    dotprod = dot(n_hat,r_hat,dim);
    DnGvjrec = -((1i*k)/4)*besselh(1,1,k.*R).*dotprod; % Projection
on normal
    Ptot(nf,ii) = Pdr(nf,ii)-sum(P.*(1i*k*beta.*Gjrec+DnGvjrec).*dl);

end
end

% SPL relative to freefield
Lp_refree = 20*log10(abs(Ptot./Pd));
Lp = 20*log10(abs(Ptot./(Pd+Pdr)));

% Insertion Loss spectra
IL = 20*log10(abs(Pdr./Ptot));

savefile=(['mat_ground_narrow_150106/BEM_Ground_narrow_Element_' num2str
(element) '_distance_' num2str(lamW) '_ElementHeight' num2str(lamH) '_
Lambda=' num2str(lam) 'm.Hz_freq:' num2str(f_start) '-' num2str(f_max)
'Hz_Nf=' num2str(Nf) '_NPPW:' num2str(NPPW) '-' datestr(DateNumber) '.
mat']);
save(savefile, 'IL', 'Lp', 'Lp_refree','N2', 'NPPW','N_CHIEF', 'P','Pd',
'Pdr', 'Pinc', 'Ptot', 'XY_CHIEF','dl','dr','f_vec','hs','n_hat','xr','xs',
'xy','zbl','zr')

clear XY_CHIEF dl n_hat xy IL Lp Lp_refree P Pd Pdr Pinc Ptot N2 DL
DRG_leg DnGv_leg DnGvji DnGvjrec G_leg Gij Gjrec N_tot R Rd Rd_chief Rr
Rr_chief Rtmp beta dotprod dotprod_leg gamma_ji n_hat_leg r_hat
r_hat_leg xy_leg
end
end
end

```

## nodesRoughnessground.m

```

% Code writted by Bart van der Aa, based on JF110524
% Adjusted for its purpose by Anna Novak

function [xy dl n_hat VEC]=nodes.Roughness_ground(c0, f_vec, NPPW, xy_vec)

% The size of each patch (max)
dl_max=(c0/max(f_vec))/NPPW;

% Describe roughness in boundary elements
xy_corner(1,:)=xy_vec(1,:);%
xy_corner(2,:)=xy_vec(2,:);

% Repeat coordinates in image-plane
xy_corner_i = xy_corner(:,2:end-1);
xy_corner_i(2,:) = xy_corner_i(2, :)*-1;
xy_corner = [xy_corner fliplr(xy_corner_i)];
xy_corner(:,end+1) = xy_corner(1:2,1); % repeat 1st coordinate

% Number of corners above ground
N_corner_tot = size(xy_corner,2);

% Create line objects
lineObject=zeros(5,N_corner_tot-1);
for ii=1:N_corner_tot-1
    lineObject(1,ii)=xy_corner(1,ii);    % x-coor 1
    lineObject(2,ii)=xy_corner(1,ii+1);  % x-coor 2
    lineObject(3,ii)=xy_corner(2,ii);    % y-coor 1
    lineObject(4,ii)=xy_corner(2,ii+1);  % y-coor 2
end

% Initialize starting value for index vector
indVecStart=0;

for ii=1:N_corner_tot-1

    lengthLine=sqrt((lineObject(1,ii)-lineObject(2,ii))^2+
        (lineObject(3,ii)-lineObject(4,ii))^2);
    N_act=ceil(lengthLine/dl_max); % Number of nodes on present
    lineObject
    dl_act=lengthLine/N_act;      % Patch size on present lineObject

    % Create node vector
    nodeVec=(1:N_act)'.5)*dl_act;

    % Determine unit-vector to obtain direction in which nodes must
    be distributed
    unitVector=( [lineObject(2,ii);lineObject(4,ii)]-[lineObject(1,ii);
    lineObject(3,ii)])*1/lengthLine;

    % Index vector
    indVec=indVecStart+1:indVecStart+N_act;

    if ne(unitVector(1),0) % if x-coordinate of unitVector is not equal
    to zero the nodes must be distributed along x-direction

```



```

        xy(indVec,1)=lineObject(1,ii)+nodeVec*unitVector(1); % Multiply
with unit-vector, i.e. -1 or 1 to add or subtract with respect
to x-coordinate
        xy(indVec,2)=lineObject(3,ii)*ones(N.act,1);
        dl(indVec,1)=dl_act;

else % y-coordinates must be distributed along y-direction

        xy(indVec,1)=lineObject(1,ii)*ones(N.act,1);
        xy(indVec,2)=lineObject(3,ii)+nodeVec*unitVector(2); % Multiply
with unit-vector, i.e. -1 or 1 to add or subtract with respect
to y-coordinate
        dl(indVec,1) = dl_act;

end

% rotate unit-vector clockwise
if unitVector(1)==0 && unitVector(2)-1==0

        n_hat(indVec,1) ==-1;
        n_hat(indVec,2) =0;

elseif unitVector(1)-1==0 && unitVector(2)==0
        n_hat(indVec,1) =0;
        n_hat(indVec,2) =1;

elseif unitVector(1)==0 && (unitVector(2)-(-1))==0

        n_hat(indVec,1) =1;
        n_hat(indVec,2) =0;

elseif (unitVector(1)-(-1))==0 && unitVector(2)==0
        n_hat(indVec,1) =0;
        n_hat(indVec,2) ==-1;
end

% Set new starting value for index vector
indVecStart = max(indVec);

end
VEC=length(dl);
end

```

The codes BEM2GrundelementsCase2.m and BEM2GrundelementsCase3.m are similar to the shown BEM2GrundelementsCase1.m

## Part 4

### BEM2Cortyard10Leg.m

```

%Code made by Anna Novak and Bart van der Aa

clc
clear all
close all

DateNumber=('7-April-2015');

%Define parameters
c0 = 340; % Speed of Sound
a = log10(28.2); b = log10(708);
f_vec = logspace(a,b,(14*3)); % Frequency vector
NPPW = 10; % Spatial sampling (points per wavelnegth)
N_leg = 10; % N-point Gauss-Legendre integration
N_CHIEF = 16; % Number of CHIEF points in total

% Receiver positions in the coryard, x and z values
xr = [9.6, 9.6, 9.6, 9.6, 9.6, 9.6, 12.8, 16, 19.2, 22.4, 25.6, 28.8, 28.8, 28.8,
      28.8, 28.8, 28.8]; % 3.6; %-[3.6]; % [5 15]; % x-coordinate receiver
zr = [17.5, 14.3, 11.1, 7.9, 4.7, 1.5, 1.5, 1.5, 1.5, 1.5, 1.5, 1.5, 4.7, 7.9,
      11.1, 14.3, 17.5]; % z-coordinate receiver

% Source position, x and z values
xs = -100; % Distance 100 m from first building
zs = 30; % Height of source

% Dimensions of the buildings
xbl = 0; % Where the first building starts in
          x-direction
xbr = 9.6; % Where the first building ends in
          x-direction
zbl = 19.2; % Height of buildings

% Dimensions of the coryard
cy=19.2; % Width of coryard

%Calculations are done in following function:
[Lp.refree, IL, Pd, Pdr, Ptot, Lp, xy] = bem2dsmallcoryardWithCHIEF(f_vec, c0,
xr, zr, xs, zs, xbl, zbl, xbr, N_leg, NPPW, N_CHIEF, cy);

% Save data
save(['mat.simple_coryard150407/BEM2D-simpleCoryard-Case3.' num2str(zbl)
'f_vec:' num2str(f_vec(1)) '-' num2str(f_vec(end)) 'Hz_xs_' num2str(xs) '_zs_'
num2str(zs) 'NPPW:' num2str(NPPW) '_N_leg:'
num2str(N_leg) '_' datestr(DateNumber) '.mat'])

```

### **bem2dsmallcoryardWithCHIEF.m**

```

%Function made by Anna Novak and Bart van der Aa

function [Lp.refree, IL, Pd, Pdr, Ptot, Lp, xy] = bem2dsmallcoryardWithCHIEF
(f_vec, c0, xr, zr, xs, zs, xbl, zbl, xbr, N_leg, NPPW, N_CHIEF, cy)

```

```

% Setup
Nf = length(f_vec);           % Number of frequencies
k_vec = 2*pi*f_vec/c0;       % Wave number

Nr = numel(xr);              % Number of receiver locations
W = abs(xbr-xbl);           % Width of building [m]
H = zbl;                     % Height of building [m]
hs = zs;                     % Source height [m]
ds = xbl-xs;                 % Horizontal distance source - screen [m]

% Prepare for pressure matrixes
Pd = zeros(Nf,Nr);          % Direct pressure
Pdr = zeros(Nf,Nr);         % Total pressure, without building
Ptot = zeros(Nf,Nr);        % Total pressure, with building

%-----
% Calculation loop for each frequency
for nf = 1:Nf

    f_vec(nf)
    k = k_vec(nf);

    % The nodes of each building is defined in following two functions
    [xy1 dl1 n_hat1]=nodes_smallcortyard-2Rough-Case1234(c0, nf, f_vec,
    NPPW, H, W, ds, cy);
    [xy2 dl2 n_hat2]=nodes_smallcortyard-0Rough(c0, nf, f_vec, NPPW, H,
    W, ds, cy);

    % Sum the nodes, elements and normal vectors from the two functions
    into the same
    % matrix
    xy(:,1)= [xy1(:,1); xy2(:,1)]; % x-parameters
    xy(:,2)= [xy1(:,2); xy2(:,2)]; % y-parameters
    dl= [dl1; dl2];                % the size of each surface elements

    %normal vectors
    n_hat(:,1)= [n_hat1(:,1); n_hat2(:,1)];
    n_hat(:,2)= [n_hat1(:,2); n_hat2(:,2)];

    N2=length(xy);                % Total ammount of elements
    N=N2/2;                         % Number of elements per building

    % 10-th order Gauss-Legendre quadrature, with position terms R_leg,
    and weight
    % terms W_leg
    N_leg=10;
    R_leg=[-0.9739 -0.8651 -0.6794 -0.4334 -0.1489 0.1489 0.4334 0.6794
    0.8651 0.9739]';
    W_leg=[0.0667 0.1495 0.2191 0.2693 0.2955 0.2955 0.2693 0.2191 0.1495
    0.0667];

    % Each element is described as 10 points from -dl/2 to dl/2. The node
    % is positioned at the centre of ech surface element

```

```

xy_leg=zeros(N2,2,N_leg);
for n=1:N2
    xy_leg(n,1,:)=xy(n,1)+.5*dl(n)*R_leg*n_hat(n,2);
    xy_leg(n,2,:)=xy(n,2)+.5*dl(n)*R_leg*n_hat(n,1);
end

% Exciting field
xy0 = [xs hs];           % Position of source
xy0Mat(1,:) = xy0;

% Distance from source to each element
Rd = sqrt(sum((xy0(ones(N2,1),:)-xy(1:N2,:)).^2,2));

xy0 = [xs -hs];         % Position of image source
xy0Mat(2,:) = xy0;

% Distance from reflection to each element
Rr = sqrt(sum((xy0(ones(N2,1),:)-xy(1:N2,:)).^2,2));

% CHIEF points

%CHIEF points in first building
XY_CHIEF(1,[1 2]) = [2.0 11.5];
XY_CHIEF(2,[1 2]) = [7.35 10.5];
XY_CHIEF(3,[1 2]) = [8.52 -0.1];
XY_CHIEF(4,[1 2]) = [5.1 -3.82];
XY_CHIEF(5,[1 2]) = [5.75 2];
XY_CHIEF(6,[1 2]) = [4.9 -4.6];
XY_CHIEF(7,[1 2]) = [7.5 17.2];
XY_CHIEF(8,[1 2]) = [1.9 -16];

%CHIEF points in second building
XY_CHIEF(9,[1 2]) = [32.0 2.5];
XY_CHIEF(10,[1 2]) = [29.35 8.5];
XY_CHIEF(11,[1 2]) = [37.52 -10.1];
XY_CHIEF(12,[1 2]) = [35.3 -18.0];
XY_CHIEF(13,[1 2]) = [32.75 14.2];
XY_CHIEF(14,[1 2]) = [34.9 -6];
XY_CHIEF(15,[1 2]) = [37.5 2];
XY_CHIEF(16,[1 2]) = [31.9 -1.5];

% Distance from direct field and reflection to each element
xy0 = xy0Mat(1,:);
Rd_chief=sqrt(sum((xy0(ones(N_CHIEF,1),:)-XY_CHIEF(1:N_CHIEF,:)).^2,2));
xy0 = xy0Mat(2,:);
Rr_chief=sqrt(sum((xy0(ones(N_CHIEF,1),:)-XY_CHIEF(1:N_CHIEF,:)).^2,2));

%-----
% Build matrix
beta=zeros(N2,1);      % admittance at boundary points

A = zeros(N2,N2);      % "transfer matrix".

```

```

% The calculation is done for each element
for m = 1:N2
    xy0=xy(m,:);

    Rtmp = reshape(sqrt((xy0(1)-xy_leg(:,1,:)).^2+(xy0(2)-
xy_leg(:,2,:)).^2),N2,N_leg);

    r_hat_leg=zeros(N2,N_leg,2);
    r_hat_leg(:,:,1) = reshape(xy0(1)-xy_leg(:,1,:),N2,N_leg)./Rtmp;
    r_hat_leg(:,:,2) = reshape(xy0(2)-xy_leg(:,2,:),N2,N_leg)./Rtmp;

    n_hat_leg=zeros(N2,N_leg,2);
    for n=1:N_leg
        n_hat_leg(:,n,:)=n_hat;
    end

    % Pressure Green's functions:
    G_leg = (1i/4)*besselh(1,1,k.*Rtmp);

    % Velocity Green's functions:
    DRG_leg = -((1i*k)/4)*besselh(1,1,k.*Rtmp);

    dim = 3; % in which matrix dimension
to take
dot product
    dotprod_leg=dot(n_hat_leg,r_hat_leg,dim);
    DnGv_leg=DRG_leg.*dotprod_leg; % projection on normal

    Gji = sum(G_leg.*W_leg(ones(N2,1),:),2)/2;
    DnGvji = sum(DnGv_leg.*W_leg(ones(N2,1),:),2)/2;

    gamma_ji = ((1i*k*beta(1:N2)).*Gji(1:N2)+DnGvji(1:N2)).*dl(1:N2).';

    A(m,:) = gamma_ji;
    A(m,m) = A(m,m)+(1/2);%1/2 due to the SHIE
end

% Build up matrix of CHIEF points
if N_CHIEF>0
    for mc = 1:N_CHIEF;
        xy0 = XY_CHIEF(mc,:); % xy0 is temporary CHIEF point

        Rtmp = reshape(sqrt((xy0(1)-xy_leg(:,1,:)).^2+(xy0(2)-
xy_leg(:,2,:)).^2), N2,N_leg);

        r_hat_leg=zeros(N2,N_leg,2);
        r_hat_leg(:,:,1)=reshape(xy0(1)-xy_leg(:,1,:),N2,N_leg)./Rtmp;
        r_hat_leg(:,:,2)=reshape(xy0(2)-xy_leg(:,2,:),N2,N_leg)./Rtmp;

        n_hat_leg=zeros(N2,N_leg,2);
        for n=1:N_leg
            n_hat_leg(:,n,:)=n_hat;
        end
    end
end

```

```

end

%% Green's functions:
G_leg = (1i/4)*besselh(0,1,k.*Rtmp); % pressure green's
function
DRG_leg = -((1i*k)/4)*besselh(1,1,k.*Rtmp); % velocity green's
function

dim = 3; % in which matrix dimension to take dot
product
dotprod_leg=dot(n_hat_leg,r_hat_leg,dim);
DnGv_leg=DRG_leg.*dotprod_leg; % projection on normal

Gji = sum(G_leg.*W_leg(ones(N2,1),:),2)/2;
DnGvj = sum(DnGv_leg.*W_leg(ones(N2,1),:),2)/2;

gamma_ji = ((1i*k*beta(1:N2)).*Gji(1:N2)+DnGvj(1:N2)).*
dl(1:N2)).';
A(N2+mc,:)=gamma_ji;

end
end

% Solve
DRG_fun = -((1i*k)/4)*besselh(1,1,k.*Rtmp); % velocity green's
function

Pinc = zeros(N2+N_CHIEF,1);
Pinc(1:N2) = (1i/4)*besselh(0,1,k.*Rd) + (1i/4)*besselh(0,1,k.*Rr);
Pinc(N2+1:end) = (1i/4)*besselh(0,1,k.*Rd_chief) + (1i/4)*
besselh(0,1,k.*Rr_chief);
P=A\Pinc;

% loop through receiver locations
for ii = 1:Nr

dr = xr(ii)-xbr; % Horizontal distance building--receiver [m]
L = ds+W+dr;
R0d = sqrt(sum(([xs hs]-[L zr(ii)])).^2));
R0r = sqrt(sum(([xs -hs]-[L zr(ii)])).^2));

Pd(nf,ii) = (1i/4)*besselh(0,1,k.*R0d);
Pdr(nf,ii) = (1i/4)*besselh(0,1,k.*R0d) + (1i/4)*besselh(0,1,k.*R0r);

xy0 = [L zr(ii)];
R = sqrt(sum((xy0(ones(N2,1),:)-xy).^2,2));

% pressure sources:
Gjrec = (1i/4)*besselh(0,1,k.*R);

% velocity sources:
r_hat = (xy0(ones(N2,1),:)-xy)./R(:,ones(1,2));

```

```

        dim = 2;
        dotprod = dot(n_hat, r_hat, dim);
        DnGvjrec = -((1i*k)/4)*besselh(1,1,k.*R).*dotprod; % Projection
on normal
        Ptot(nf,ii) = Pdr(nf,ii)-sum(P.*(1i*k*beta.*Gjrec+DnGvjrec).*dl);

    end
end
%%
%----
% plot:
    figure(1)
    axis equal
    hold on
    groundplot_x=-111:0.5:50; %To make the ground in the plot
    groundplot_y=zeros(1,length(groundplot_x));
    figure(1)
    for n=1:N2
        plot(reshape(xy_leg(n,1,:),1,N_leg),reshape(xy_leg(n,2,:),
1,N_leg),'k')
        hold on
    end
    plot(xr,zr,'bo',xs,zs,'ro')
    axis([xs-5 40 0 35])

    plot(groundplot_x, groundplot_y,'k')

%----

%% Post processing

% SPL relative to freefield
Lp_refree = 20*log10(abs(Ptot./Pd));
Lp= 20*log10(abs(Ptot./(Pd+Pdr)));

% Insertion Loss spectra
IL = 20*log10(abs(Pdr./Ptot));

```

### **nodes smallcortyard2RoughCase1234.m**

```

function [xy dl n_hat]=nodes_smallcortyard_2Rough_Case1234(c0, nf, f_vec,
NPPW, H, W, ds, cy);

%Overall parameters:
dl_max=(c0/max(f_vec))/NPPW;
Nf=length(f_vec);
k_vec=2*pi*f_vec/c0;

% Describe building in boundary elements

```

```

%-----
%Four different cases, choose here:
[xy_corner] = Func_corners_case1();
%[xy_corner] = Func_corners_case2();
%[xy_corner] = Func_corners_case3();
%[xy_corner] = Func_corners_case4();
%-----

% Repeat coordinates in image-plane
xy_corner_i = xy_corner(:,2:end-1);
xy_corner_i(2,:) = xy_corner_i(2,:)*-1;
xy_corner = [xy_corner fliplr(xy_corner_i)];
xy_corner(:,end+1) = xy_corner(1:2,1); % repeat 1st coordinate

% Number of corners above ground
N_corner_tot = size(xy_corner,2);

% Create 4D line-object
lineObject=zeros(5,N_corner_tot-1);
for ii=1:N_corner_tot-1
    lineObject(1,ii)=xy_corner(1,ii);    % x-coor 1
    lineObject(2,ii)=xy_corner(1,ii+1); % x-coor 2
    lineObject(3,ii)=xy_corner(2,ii);    % y-coor 1
    lineObject(4,ii)=xy_corner(2,ii+1); % y-coor 2
end

% Initialize starting value for index vector
indVecStart=0;
for ii=1:N_corner_tot-1

    lengthLine=sqrt((lineObject(1,ii)-lineObject(2,ii))^2+(lineObject(3,ii)
-lineObject(4,ii))^2);
    N_act=ceil(lengthLine/dl_max); % Number of nodes on present lineObject
    dl_act=lengthLine/N_act;      % Patch-size on present lineObject

    % Create node vector
    nodeVec=(1:N_act)'.5*dl_act;

    % Determine unit-vector to obtain direction in which nodes must be
distributed
    unitVector=( [lineObject(2,ii);lineObject(4,ii)]-[lineObject(1,ii);
lineObject(3,ii)]) *1/lengthLine;

    % Index vector
    indVec=indVecStart+1:indVecStart+N_act;

    if ne(unitVector(1),0) % if x-coordinate of unitVector is not equal
to zero the nodes must be distributed along x-direction

        xy(indVec,1)=lineObject(1,ii)+nodeVec*unitVector(1); % Multiply
with unit-vector, i.e. -1 or 1 to add or subtract with respect
to x-coordinate
        xy(indVec,2)=lineObject(3,ii)*ones(N_act,1);
        dl(indVec,1)=dl_act;
    end
end
end

```



```

else % y-coordinates must be distributed along y-direction

    xy(indVec,1)=lineObject(1,ii)*ones(N.act,1);
    xy(indVec,2)=lineObject(3,ii)+nodeVec*unitVector(2); % Multiply
with unit-vector, i.e. -1 or 1 to add or subtract with respect
to y-coordinate
    dl(indVec,1) = dl_act;

end

% rotate unit-vector clockwise
if unitVector(1)==0 && unitVector(2)-1==0

    n_hat(indVec,1) =-1;
    n_hat(indVec,2) =0;

elseif unitVector(1)-1==0 && unitVector(2)==0
    n_hat(indVec,1) =0;
    n_hat(indVec,2) =1;

elseif unitVector(1)==0 && (unitVector(2)-(-1))==0

    n_hat(indVec,1) =1;
    n_hat(indVec,2) =0;

elseif (unitVector(1)-(-1))==0 && unitVector(2)==0
    n_hat(indVec,1) =0;
    n_hat(indVec,2) =-1;
end

% Set new starting value for index vector
indVecStart = max(indVec);

end

end

```

### **bnodes smallcortyard 0Rough.m**

```

function [xy dl n_hat]=nodes-smallcortyard.0Rough(c0, nf, f_vec, NPPW, H,
W, ds, cy);

dl_max=(c0/max(f_vec))/NPPW;

% Describe building in boundary elements

xy_corner=[28.8,0;
%          28.8,0.64; %+0.64
%          28.96,0.64;
%          28.96,2.56; %+1.92

```

```

%      28.8,2.56;
%      28.8,3.84;%+1.28
%      28.96,3.84;
%      28.96,5.76;
%      28.8,5.76;
%      28.8,7.04;
%      28.96,7.04;
%      28.96,8.96;
%      28.8,8.96;
%      28.8,10.24;
%      28.96,10.24;
%      28.96,12.16;
%      28.8,12.16;
%      28.8,13.44;
%      28.96,13.44;
%      28.96,15.36;
%      28.8,15.36;
%      28.8,16.64;
%      28.96,16.64;
%      28.96,18.56;
%      28.8,18.56;
      28.8,19.2;% Here starts the roof!
38.4,19.2;
%      38.4,18.56;
%      9.44,18.56;
%      9.44,16.64;
%      38.4,16.64;
%      38.4,15.36;
%      9.44,15.36;
%      9.44,13.44;
%      38.4,13.44;
%      38.4,12.16;
%      9.44,12.16;
%      9.44,10.24;
%      38.4,10.24;
%      38.4,8.96;
%      9.44,8.96;
%      9.44,7.04;
%      38.4,7.04;
%      38.4,5.76;
%      9.44,5.76;
%      9.44,3.84;
%      38.4,3.84;
%      38,2.56;
%      9.44,2.56;
%      9.44,0.64;
%      9.6,0.64;
38.4,0].';

```

```

% Number of corners above ground
N_corner = size(xy_corner,2);

% Repeat coordinates in image-plane

```

```

xy_corner_i = xy_corner(:,2:end-1);
xy_corner_i(2,:) = xy_corner_i(2, :)*-1;
xy_corner = [xy_corner fliplr(xy_corner_i)];
xy_corner(:,end+1) = xy_corner(1:2,1); % repeat 1st coordinate

% Number of corners above ground
N_corner_tot = size(xy_corner,2);

% Create 4D line-object, which later can be used to define impedance
% surfaces too
lineObject=zeros(5,N_corner_tot-1);
for ii=1:N_corner_tot-1
    lineObject(1,ii)=xy_corner(1,ii);    % x-coor 1
    lineObject(2,ii)=xy_corner(1,ii+1); % x-coor 2
    lineObject(3,ii)=xy_corner(2,ii);    % y-coor 1
    lineObject(4,ii)=xy_corner(2,ii+1); % y-coor 2
end

% Initialize starting value for index vector
indVecStart=0;
for ii=1:N_corner_tot-1

    lengthLine=sqrt((lineObject(1,ii)-lineObject(2,ii))^2+(lineObject(3,ii)
-lineObject(4,ii))^2);
    N_act=ceil(lengthLine/dl_max); % Number of nodes on present lineObject
    dl_act=lengthLine/N_act;      % Patch-size on present lineObject

    % Create node vector
    nodeVec=(1:N_act)'.5)*dl_act;

    % Determine unit-vector to obtain direction in which nodes must be
    distributed
    unitVector=( [lineObject(2,ii);lineObject(4,ii)]-[lineObject(1,ii);
lineObject(3,ii)])*1/lengthLine;

    % Index vector
    indVec=indVecStart+1:indVecStart+N_act;

    if ne(unitVector(1),0) % if x-coordinate of unitVector is not equal to
zero the nodes must be distributed along x-direction

        xy(indVec,1)=lineObject(1,ii)+nodeVec*unitVector(1); % Multiply with
unit-vector, i.e. -1 or 1 to add or subtract with respect to
x-coordinate
        xy(indVec,2)=lineObject(3,ii)*ones(N_act,1);
        dl(indVec,1)=dl_act;
        % add beta
    else % y-coordinates must be distributed along y-direction

        xy(indVec,1)=lineObject(1,ii)*ones(N_act,1);
        xy(indVec,2)=lineObject(3,ii)+nodeVec*unitVector(2); % Multiply with
unit-vector, i.e. -1 or 1 to add or subtract with respect to
y-coordinate
        dl(indVec,1) = dl_act;
    end
end

```

```

        % add beta
    end

    % rotate unit-vector clockwise

    if unitVector(1)==0 && unitVector(2)-1==0

        n_hat(indVec,1) =-1;
        n_hat(indVec,2) =0;

    elseif unitVector(1)-1==0 && unitVector(2)==0
        n_hat(indVec,1) =0;
        n_hat(indVec,2) =1;

    elseif unitVector(1)==0 && (unitVector(2)-(-1))==0

        n_hat(indVec,1) =1;
        n_hat(indVec,2) =0;

    elseif (unitVector(1)-(-1))==0 && unitVector(2)==0
        n_hat(indVec,1) =0;
        n_hat(indVec,2) =-1;
    end

    % Set new starting value for index vector
    indVecStart = max(indVec);

end

end

```

### **Funcornerscase1.m**

```

function[xy_corner]=Func_corners_case1()

%Element parameters
dd=0.2057;
q=0.85;
ww=q*1.6;

xy_corner=[0,0;
%           0,0.64; %+0.64 %For a non flat facade
%           0.16,0.64;
%           0.16,2.56; %+1.92
%           0,2.56;
%           0,3.84; %+1.28
%           0.16,3.84;
%           0.16,5.76;
%           0,5.76;
%           0,7.04;
%           0.16,7.04;

```

```

%           0.16,8.96;
%           0,8.96;
%           0,10.24;
%           0.16,10.24;
%           0.16,12.16;
%           0,12.16;
%           0,13.44;
%           0.16,13.44;
%           0.16,15.36;
%           0,15.36;
%           0,16.64;
%           0.16,16.64;
%           0.16,18.56;
%           0,18.56;
0,19.2;% Here starts the roof! Add roughness here!
dd,19.2;
dd,18.35;
(dd+ww),18.35;
(dd+ww),19.2;
(dd*2+ww),19.2;
(dd*2+ww),18.35;
(dd*2+ww*2),18.35;
(dd*2+ww*2),19.2;
(dd*3+ww*2),19.2;
(dd*3+ww*2),18.35;
(dd*3+ww*3),18.35;
(dd*3+ww*3),19.2;
(dd*4+ww*3),19.2;
(dd*4+ww*3),18.35;
(dd*4+ww*4),18.35;
(dd*4+ww*4),19.2;
(dd*5+ww*4),19.2;
(dd*5+ww*4),18.35;
(dd*5+ww*5),18.35;
(dd*5+ww*5),19.2;
(dd*6+ww*5),19.2;
(dd*6+ww*5),18.35;
(dd*6+ww*6),18.35;
(dd*6+ww*6),19.2;
9.6,19.2;
%           9.6,18.56;
%           9.44,18.56;
%           9.44,16.64;
%           9.6,16.64;
%           9.6,15.36;
%           9.44,15.36;
%           9.44,13.44;
%           9.6,13.44;
%           9.6,12.16;
%           9.44,12.16;
%           9.44,10.24;
%           9.6,10.24;
%           9.6,8.96;
%           9.44,8.96;

```

```
%      9.44,7.04;  
%      9.6,7.04;  
%      9.6,5.76;  
%      9.44,5.76;  
%      9.44,3.84;  
%      9.6,3.84;  
%      9.6,2.56;  
%      9.44,2.56;  
%      9.44,0.64;  
%      9.6,0.64;  
%      9.6,0] .';
```

The codes `Funccornerscase2.m`, `Funccornerscase3.m` and `Funccornerscase4.m` are similar to the shown `Funccornerscase1.m`